

Catalytic Intermolecular Asymmetric $[2\pi + 2\sigma]$ Cycloadditions of Bicyclo[1.1.0]butanes: Practical Synthesis of Enantioenriched Highly Substituted Bicyclo[2.1.1]hexanes

Ying-Jie Li,^{||} Zhi-Long Wu,^{||} Qiang-Shuai Gu,^{||} Tingting Fan,^{||} Ming-Hao Duan, Lihong Wu, Yu-Tao Wang, Ji-Peng Wu, Fang-Lei Fu, Fan Sang, Ai-Ting Peng, Yuyang Jiang,^{*} Xin-Yuan Liu,^{*} and Jin-Shun Lin^{*}



Cite This: <https://doi.org/10.1021/jacs.4c10968>



Read Online

ACCESS |



Metrics & More

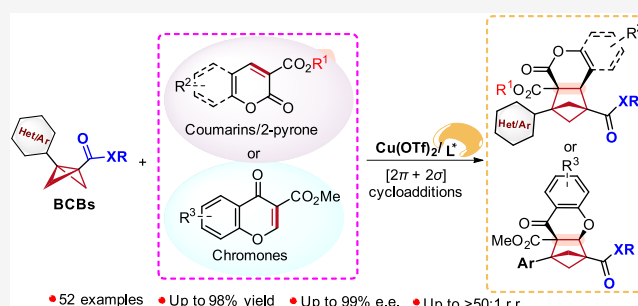


Article Recommendations



Supporting Information

ABSTRACT: The high percentage of sp^3 -hybridized carbons and the presence of chiral carbon centers could contribute to increased molecular complexity, enhancing the likelihood of clinical success of drug candidates. Three-dimensional (3D) bridged motifs have recently garnered significant interest in medicinal chemistry. Bicyclo[2.1.1]hexanes (BCHs) are emerging 3D benzene bioisosteres, but the synthesis of chiral, highly substituted BCHs has been underexplored. Herein, we disclose the Lewis acid-catalyzed asymmetric intermolecular $[2\pi + 2\sigma]$ cycloaddition of bicyclo[1.1.0]butanes with coumarins, 2-pyrone, or chromones to access diverse enantioenriched 1,2,3,4-tetrasubstituted BCHs bearing vicinal tertiary-quaternary stereocenters. The key to success is the introduction of chiral bisoxazoline ligands to effectively suppress the side reactions, inhibit significant racemic background reactions, and fine-tune the reactivity and regio-, enantio-, and diastereoselectivities of the reactions. The resulting BCHs hold significant potential as benzene bioisosteres in the synthesis of chiral BCHex-Sonidegib and BCHex-BMS-202, mimicking the anticancer drug Sonidegib and the PD-1/PD-L1 inhibitor BMS-202, respectively. The outcome highlights the positive impact of bioisosteric replacement on physicochemical properties, while maintaining comparable antitumor activity to their aryl-containing counterparts.



INTRODUCTION

The concept of “escaping flatland” has recently been widely acknowledged by medicinal chemists, emphasizing molecular complexity as a critical parameter in drug design.¹ The fraction of sp^3 -hybridized carbons (F_{sp^3})² and the presence of chiral carbon centers are two key descriptors to quantify the molecular complexity,³ and higher molecular complexity could increase the probability of clinical success of drug candidates.^{1a} As an increase in F_{sp^3} could result in higher molecular complexity, replacing planar arenes with three-dimensional (3D) motifs has recently garnered significant interest. Among these captivating 3D motifs,⁴ particularly the bicyclo[1.1.1]pentanes,⁵ bicyclo[2.1.1]-hexanes (BCHs),⁶ bicyclo[3.1.1]heptanes (BCHeps),⁷ and cubanes⁸ emerge as benzene bioisosteres.⁹ They present diverse distinguishing physicochemical properties,^{1–3} including improved metabolic stability, fewer off-target effects, and enhanced selectivity via better interaction with the biological targets. Of particular interest is the BCHs motif (Scheme 1A), which could act as bioisosteres of diverse substituted benzenes in active pharmaceutical ingredients¹⁰ (Figure S1 in the SI). In addition to F_{sp^3} , a higher number of stereogenic centers could also

enhance molecular complexity.^{1a} Clear evidence indicates that chiral motifs, especially those with quaternary carbon stereocenters,¹¹ could significantly enhance molecular recognition to exhibit better selectivity. Consequently, drug candidates with chiral centers have a lower rate of attrition in clinical trials.^{1b} However, the use of chiral all-carbon BCHs as benzene bioisosteres in drug design has been underexplored. Thus, developing a practical and versatile approach to access these motifs with multiple stereogenic centers is increasingly valuable in medicinal chemistry.

Currently, several state-of-the-art approaches exist to access all-carbon BCHs¹² (Figure S2 in the SI): (1) Ring contraction.¹³ (2) Thermo-driven cycloadditions of bicyclo[1.1.0]butanes (BCBs).¹⁴ (3) The intermolecular cycloadditions of BCBs with phenols,¹⁵ bicyclic aza-arenes,¹⁶

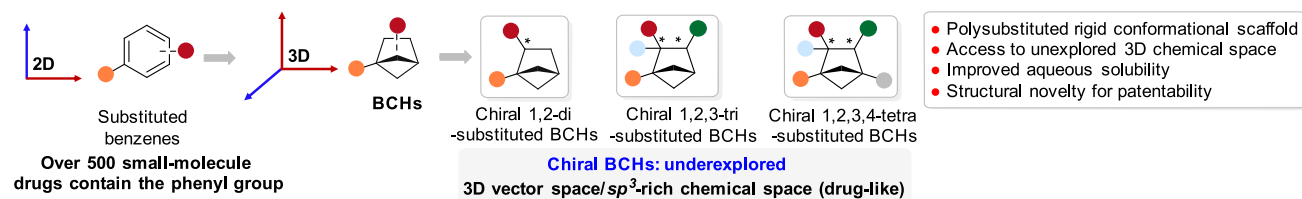
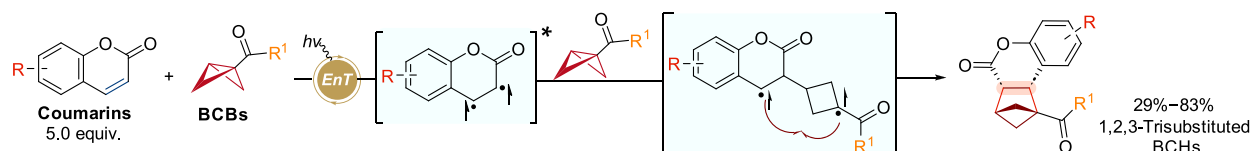
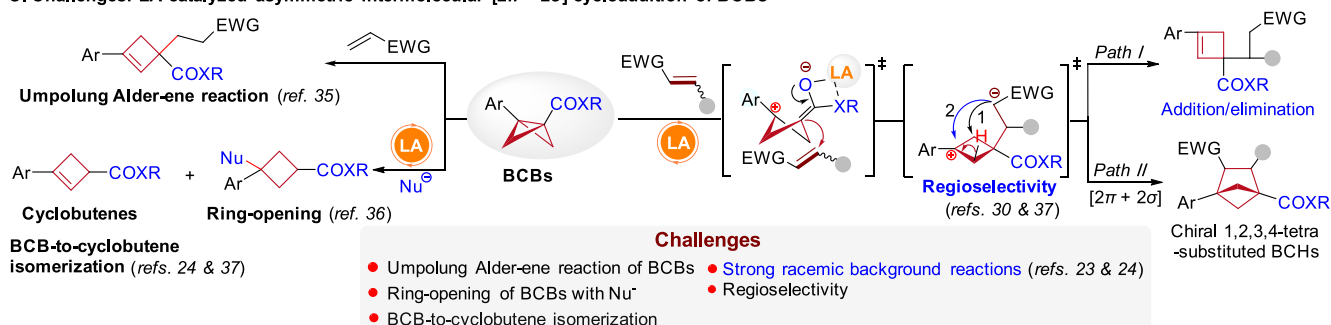
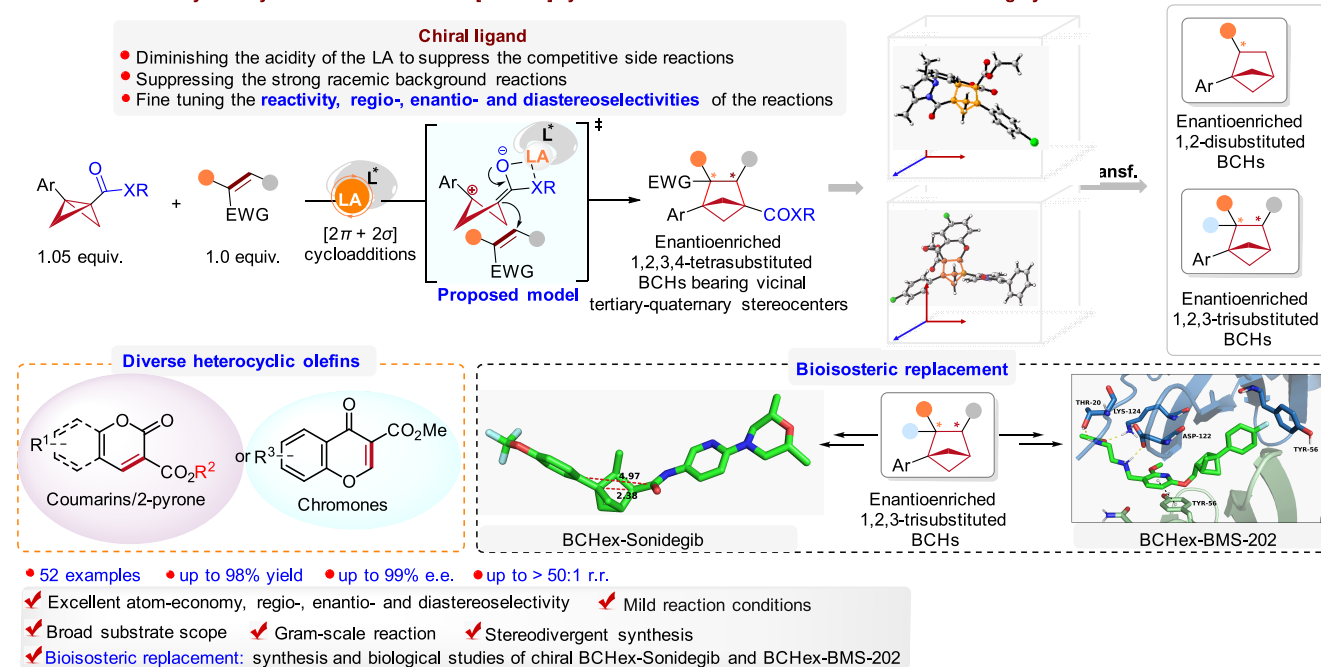
Received: August 10, 2024

Revised: October 21, 2024

Accepted: November 13, 2024

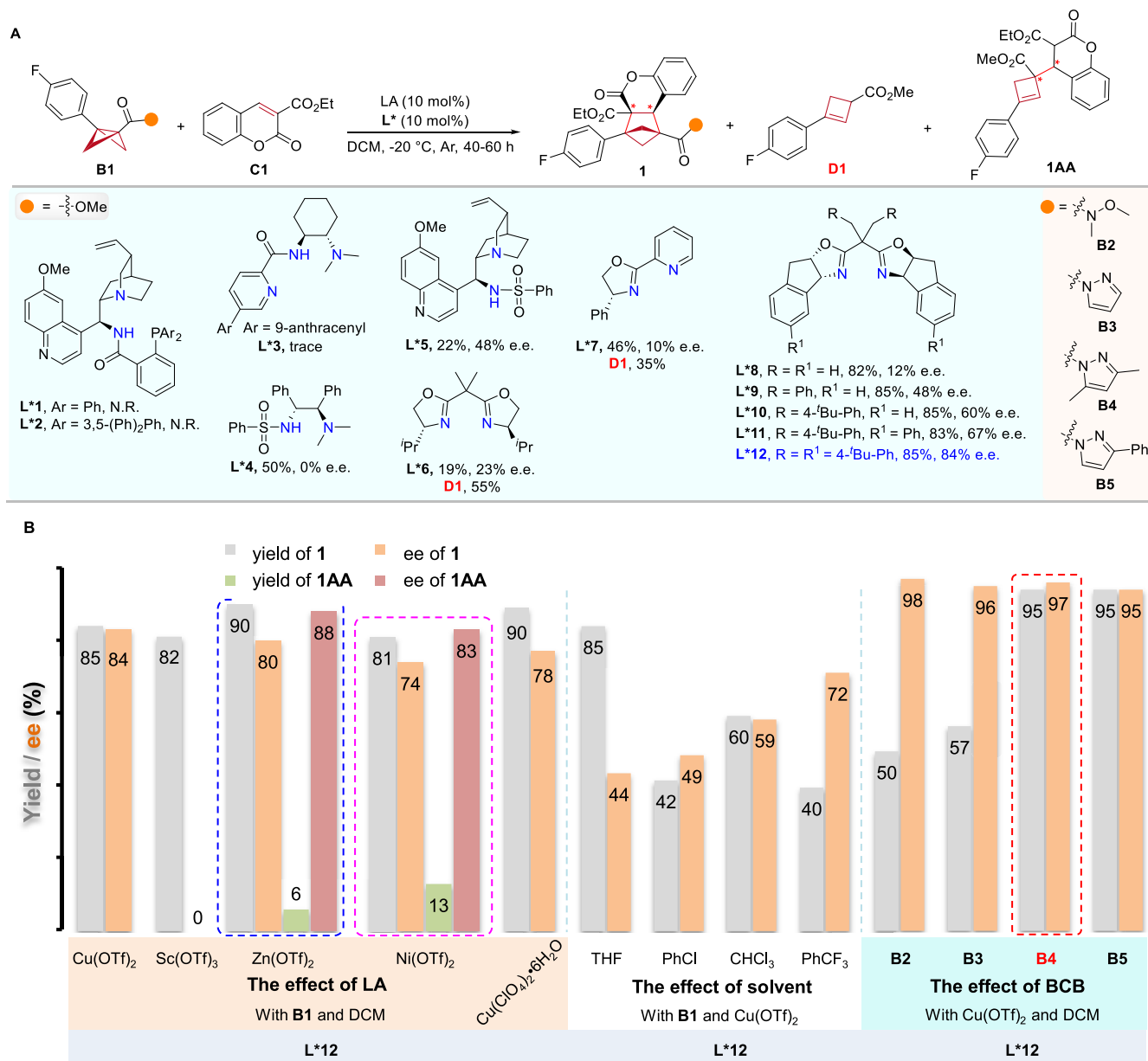
Scheme 1. LA-Catalyzed Asymmetric Intermolecular $[2\pi + 2\sigma]$ Cycloaddition of BCBs to Access Chiral Highly Substituted BCHs

A. Escape-from-flatland: chiral substituted BCHs as bioisosteres of substituted benzenes have been underexplored

B. Intermolecular $[2\pi + 2\sigma]$ -photocycloaddition of BCBs with coumarins enabled by triplet energy transfer (Glorius 2022, ref. 6b)C. Challenges: LA-catalyzed asymmetric intermolecular $[2\pi + 2\sigma]$ cycloaddition of BCBsD: This work: LA-catalyzed asymmetric intermolecular $[2\pi + 2\sigma]$ cycloaddition of BCBs to access enantioenriched highly substituted BCHs

1,3-dienes,¹⁷ or alkenes¹⁸ have been explored via radical pathways.¹⁹ Notably, Glorius' group has disclosed an elegant $[2\pi + 2\sigma]$ photocycloaddition of BCBs with coumarins, enabling access to 1,2,3-trisubstituted BCHs (Scheme 1B).^{6b} Other advances include pyridine-boryl radical-catalyzed cycloadditions reported by Li²⁰ and Wang,²¹ as well as SmI_2 -catalyzed reactions developed by Procter.^{6c} (4) Lewis acid

(LA)-catalyzed cycloadditions of BCBs with ketenes or indoles initiated by Studer,²² Deng,²³ and Feng.²⁴ (5) The intramolecular crossed photocycloaddition of 1,5-dienes developed by Mykhailiuk,^{6a,25} Walker,²⁶ and Brown.^{13,27} Unfortunately, the highly reactive BCBs are prone to generating several side reactions. Thus, most of these reactions require 1.5–3.0 equiv of BCBs or 2.0–5.0 equiv of olefins to achieve satisfactory

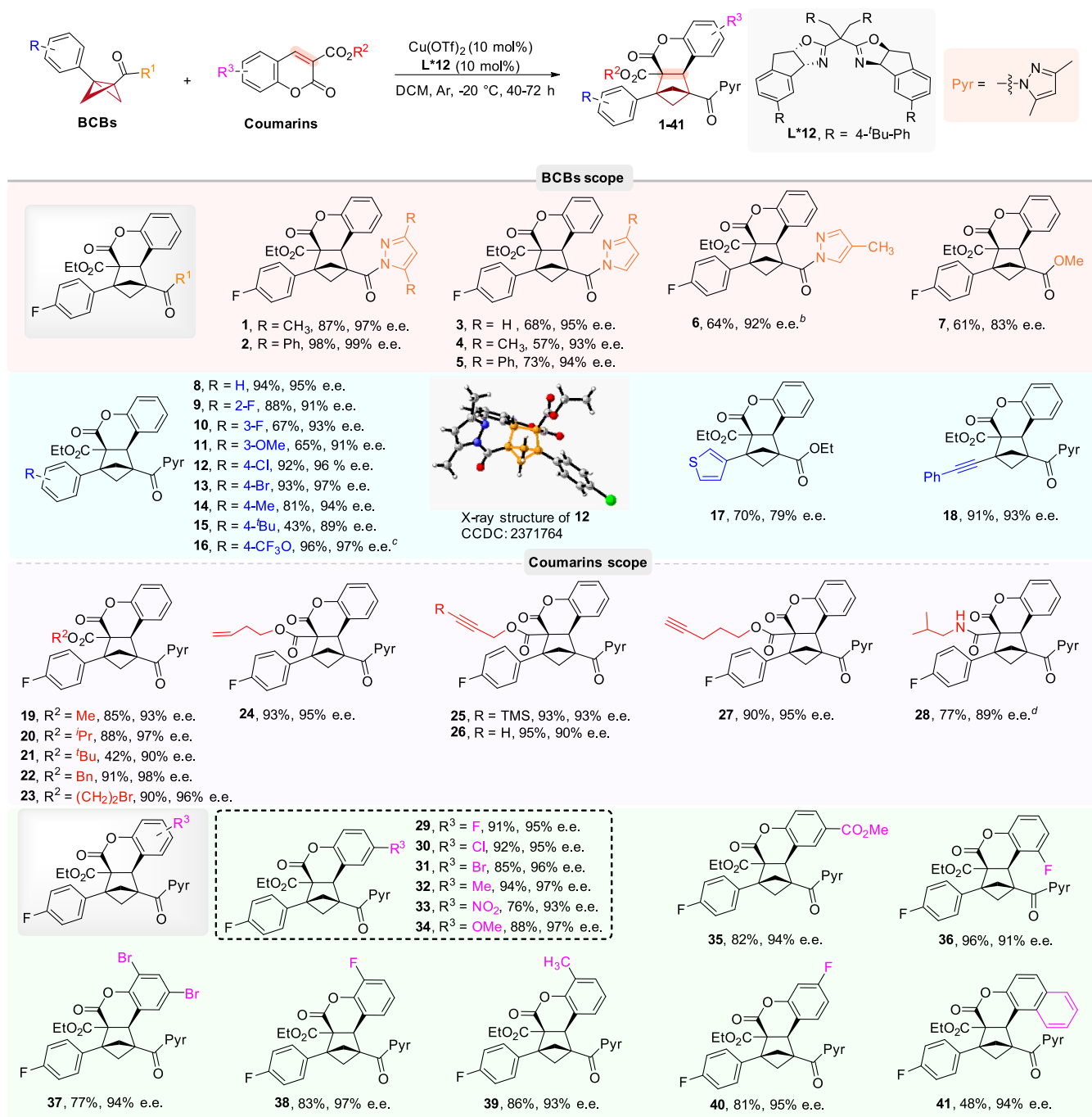
Table 1. Reaction Development and Optimization Studies^a

^aReaction development and optimization studies. Reaction conditions: **B1** (0.0525 mmol, 1.05 equiv), **C1** (0.050 mmol), LA (10 mol %), ligand (10 mol %) in DCM (0.50 mL) at $-20\text{ }^{\circ}\text{C}$ for 40–60 h under argon; Yield of **1** is based on ¹H NMR analysis of the crude product using CH₂Br₂ as an internal standard; E.e. values were based on chiral HPLC analysis.

results (Figure S2 in the SI). Recently, Bach's group²⁸ has pioneered the enantioselective $[2\pi + 2\sigma]$ photocycloaddition of BCBs with 2(1*H*)-quinolones using 2.0 equiv of the chiral catalyst. While preparing this manuscript, Jiang's group²⁹ has developed enantioselective $[2\pi + 2\sigma]$ photocycloadditions of BCBs with specifically configured vinylazaarenes to yield chiral substituted BCHs. Very recently, enantioselective cycloadditions of BCBs with vinyl oxiranes,³⁰ pyridinium 1,4-zwitterionic thiolates,³¹ azomethine ylides,³² nitrones,³³ and aromatic azomethine imines³⁴ have been developed to access chiral 2-thia-5-azabicyclo[5.1.1]nonenes, as well as oxo- or aza-BCHeps. Despite these achievements, the enantioselective $[2\pi + 2\sigma]$ cycloaddition of BCBs with high atom economy to access chiral, highly substituted all-carbon BCHs still remains largely underexplored (Scheme 1A), limiting the exploration of

previously uncharted 3D chemical space in drug discovery. Thus, the pursuit of alternative, mechanistically distinct catalytic asymmetric strategies for the cycloadditions of BCBs with easily accessible α,β -unsaturated carbonyl compounds^{6b} to produce chiral, highly substituted BCHs in an atom-economical fashion remains highly desirable.

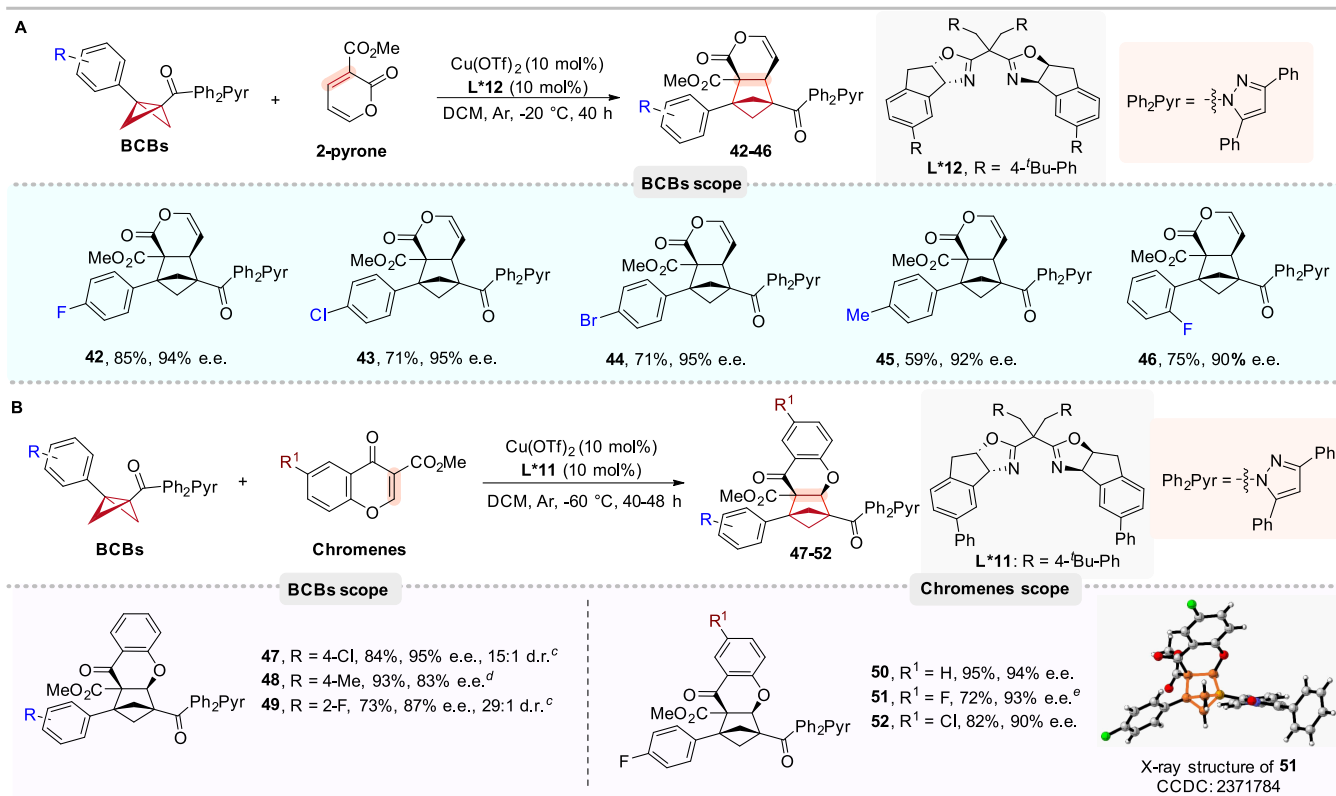
Given the significant advances in LA-catalyzed cycloaddition of BCBs,^{12a} there is a pressing need to develop corresponding asymmetric transformations to produce enantioenriched, highly substituted BCHs. To the best of our knowledge, these transformations have not yet been achieved. We envision that an LA/chiral ligand catalytic system might address this challenge (Scheme 1D). Such a system is expected to diminish the acidity of the LA to suppress competitive side reactions, inhibit strong racemic background reactions, and fine-tune the

Table 2. Substrate Scope for BCBs and Coumarins^a

^aReaction conditions: BCB (0.21 mmol, 1.05 equiv), coumarin (1.0 equiv), Cu(OTf)₂ (10 mol %), and L*12 (10 mol %) in DCM (2.0 mL) at -20 °C for 40–72 h under argon. Isolated yields for products after chromatographic separation are shown; E.e. is based on chiral HPLC analysis. ^b0 °C; ^cWith L*12 (7.5 mol %), Cu(OTf)₂ (7.5 mol %), at a 1.8 mmol scale; ^d25 °C.

reactivity and regio-, enantio-, and diastereoselectivities of the reactions. Considering the inherent instability and high reactivity of BCBs due to their high-strain energy,¹² several formidable challenges need to be addressed (Scheme 1C), including: (1) umpolung Alder-ene reaction,³⁵ (2) ring-opening reaction,³⁶ (3) BCB-to-cyclobutene isomerization,^{24,37} (4) strong racemic background reaction,^{23,24} and (5) regioselectivity issues.^{30,37} More importantly, the construction of BCHs bearing congested vicinal tertiary-quaternary carbon centers with excellent enantio- and diastereoselectivities also

constitutes a formidable challenge.³⁸ Consistent with our continuous efforts in copper-catalyzed asymmetric reactions,³⁹ we herein disclose the LA-catalyzed asymmetric intermolecular [2 π + 2 σ] cycloadditions of BCBs with coumarins, 2-pyrone, or chromenes to access the sought-after enantioenriched 1,2,3,4-tetrasubstituted BCHs. This transformation simultaneously creates vicinal tertiary-quaternary stereocenters with excellent atom economy, as well as high regio-, enantio-, and diastereoselectivities. Further transformations of the resulting BCHs lead to 1,2-di- or 1,2,3-trisubstituted BCHs. Moreover,

Table 3. Substrate Scope for BCBs with 2-Pyrone^a or Chromenes^b

^aReaction conditions: BCB (0.21 mmol, 1.05 equiv), 2-pyrone (1.0 equiv), Cu(OTf)₂ (10 mol %), and L*12 (10 mol %) in DCM at -20 °C for 40 h under argon. Isolated yields for products after chromatographic separation are shown; E.e. is based on chiral HPLC analysis. ^bReaction conditions: BCB (0.21 mmol, 1.05 equiv), chromenes (1.0 equiv), Cu(OTf)₂ (10 mol %), and L*11 (10 mol %) in DCM at -60 °C for 40–48 h under argon. Isolated yields for products after chromatographic separation are shown; E.e. is based on chiral HPLC analysis. ^cDiastereomeric ratio determined from the ¹H NMR spectra of the crude product. ^dL*12. ^eNaBAR₄^F (20 mol %) as an additive.

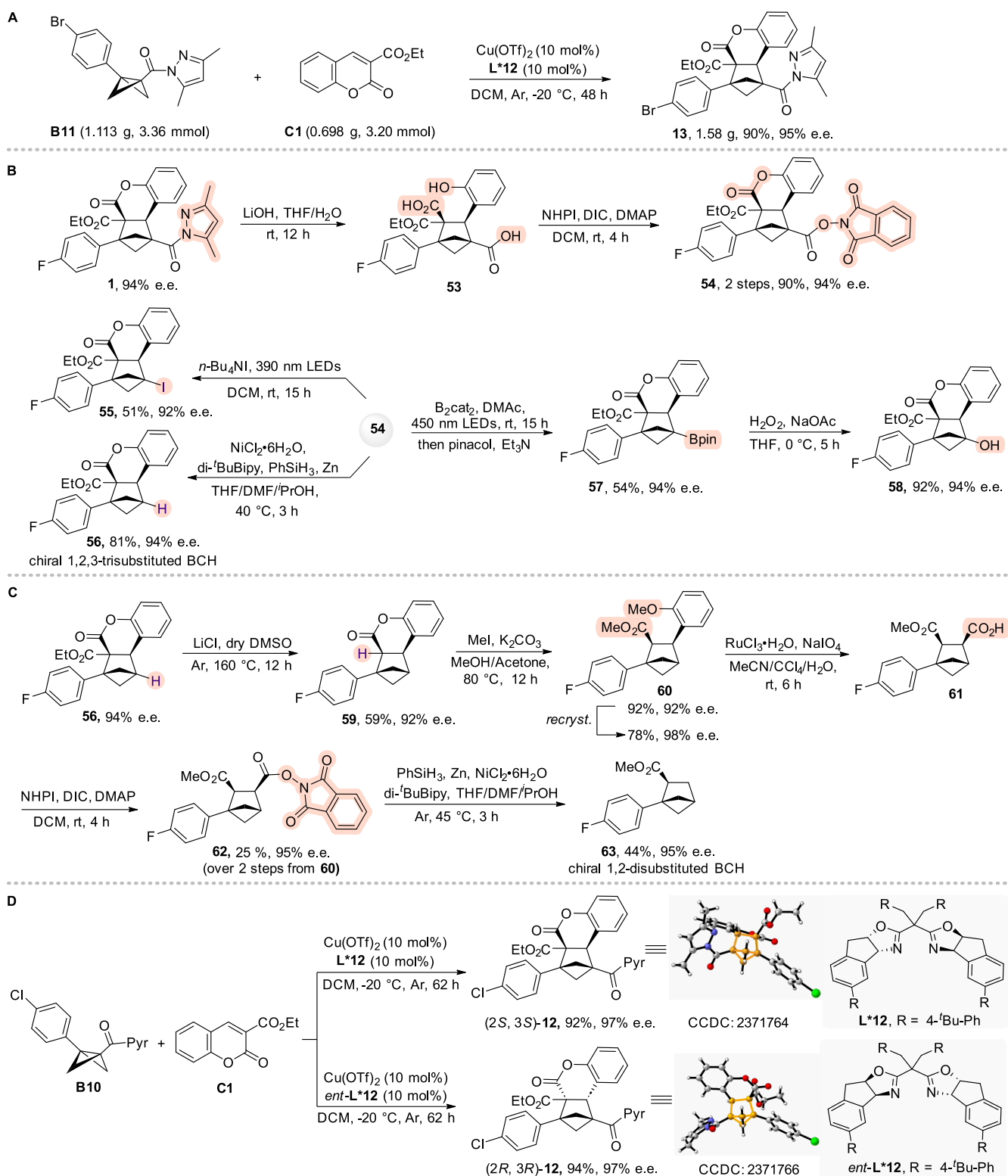
chiral BCHex-Sonidegib, an analogue of the anticancer drug Sonidegib,⁴⁰ and chiral BCHex-BMS-202, an analogue of the PD-1/PD-L1 inhibitor BMS-202,⁴¹ were synthesized. Both compounds exhibited improved physicochemical properties, while maintaining antitumor activity comparable to their aryl-containing counterparts (Scheme 1D).

RESULTS AND DISCUSSION

Reaction Development. Inspired by the pioneering photochemical [2π + 2σ] cycloadditions of BCBs with coumarins by the Glorius group^{6b} and the observation by the Leitch group³⁷ that the addition of 2,6-lutidine could inhibit the decomposition of BCBs in the presence of an LA catalyst, we initially investigated the ligand effects on the [2π + 2σ] cycloaddition of BCB **B1** with coumarin **C1**. Various types of chiral chelating *N,N,P*-, *N,N,N*-, or *N,N*-ligands (L*1–L*5)^{39c,e,42} were screened in the presence of Cu(OTf)₂ in CH₂Cl₂ (DCM) at -20 °C for 40 h under argon (Tables 1A and S1 in the SI). The tridentate *N,N,P*- and *N,N,N*-ligands (L*1–L*3) failed to initiate the reaction, leaving **B1** intact. To our delight, the use of bidentate *N,N*-ligands (L*4 and L*5) could afford the desired BCH in low to moderate yield with excellent regio- and diastereoselectivities, albeit with moderate enantioselectivity (48% e.e. for L*5). These results indicated that chiral ligands were crucial for the reactivity and stereoselection. The tridentate ligands might bind too tightly to the LA, hindering its ability to activate the BCB substrate. In

contrast, bidentate ligands appear to effectively tune the reactivity as well as the regio-, enantio-, and diastereoselectivities of the reaction. Encouraged by the results, we then switched to evaluate the commonly used chiral oxazoline-based bidentate ligands (L*6–L*12, Table 1A). L*6 and L*7 could also initiate this reaction to deliver the desired BCH in low to moderate yield with low enantioselectivity, along with the byproduct cyclobutene **D1** via bicyclobutane-to-cyclobutene isomerization. Remarkably, the Indane-derived bisoxazoline (Box) ligands (L*9–L*12) stood out in terms of both yield and e.e., and L*10 containing a 4-^tBu-Ph group afforded the desired product with excellent yield and moderate enantioselectivity (60% e.e., Table 1A). Subsequent investigation focused on optimizing the spacer on the backbone of the Box ligands. L*11 and L*12 bearing sterically bulky substituents⁴³ were synthesized to create a more defined chiral environment. Fortunately, L*12 bearing two 4-^tBu-Ph groups proved to be the most effective in promoting reactivity and enantioinduction (84% e.e., Table 1A). Subsequent evaluation of various LAs and solvents revealed that the choice of the LA catalyst and solvent strongly influenced both the yield and enantioselectivity of the reaction (Tables 1B and S2 and S3 in the SI). Moreover, the cyclobutenyl oxochromane **IAA** was observed as a byproduct via an addition/elimination process when Zn(OTf)₂ or Ni(OTf)₂ was used with L*12, consistent with previous reports.^{37,44} Inspired by the enhanced reactivity of acyl pyrazole groups⁴⁴ and their bidentate coordination mode with LAs,⁴⁵ we noted that **B3**–**B5** significantly improved

Scheme 2. Synthetic Utility



reactivity compared to the corresponding ester **B1** and amide **B2**. In particular, the use of acyl pyrazole substrate **B4** resulted in a remarkable improvement in both yield and enantioselectivity (Tables 1B and S4 in the SI). Notably, premixing the LA and chiral Box ligand in DCM was essential to prevent the rapid decomposition of BCBs in some instances.

Substrate Scope for BCBs and Coumarins. With the optimal reaction conditions established, we next investigated the substrate scope of the LA-catalyzed asymmetric $[2\pi + 2\sigma]$ cycloaddition of BCBs with coumarins (Table 2). Initially, several BCB substrates with acyl pyrazole or ester groups were investigated, delivering the corresponding BCHs 1–7 in 57–

98% yields with 83–99% e.e. Next, a series of BCB substrates with various substituents on the aromatic ring were investigated. The results indicated that both the position and electronic nature of the substituents on the aromatic ring (R) had a negligible effect on the reaction efficiency and stereoselectivity. A range of diversely functionalized BCBs, including those having phenyl groups with electron-donating (OMe, Me, and ^tBu) or electron-withdrawing (F, Cl, Br, and OCF₃) substituents at different positions (*ortho*, *meta*, or *para*), proved to be suitable substrates to furnish the expected BCHs **8–16** in 43–96% yields with 89–97% e.e. Notably, the halo-substituted BCHs offer opportunities for further useful transformations. The absolute configuration of (*S,S*)-**12** was determined by X-ray crystallographic analysis (Figure S3 in the SI). It is particularly noteworthy that 3-thiophene- and phenylacetylene-substituted BCBs, which were previously very challenging to obtain⁴⁶ and are reported here for the first time, delivered the corresponding BCHs **17** and **18**, with the additional triple bond intact, in 70–91% yields with 79–93% e.e. However, the alkynyl group in the phenylacetylene-substituted BCBs could have easily reacted with highly reactive radical intermediates in related radical processes. The novel BCHs **17** and **18** open new opportunities to explore diverse 3D chemical space in drug design. Additionally, the reduction of **18** could give a styrene-containing BCH, serving as a bioisostere for stilbene.¹⁷ Next, attention was then turned to coumarins, a privileged scaffold widely present in natural products and various drugs.⁴⁷ Under almost identical reaction conditions, coumarin substrates bearing diverse esters or amide groups were also well tolerated, affording BCHs **19–28** in 42–95% yields with excellent enantioselectivity. Notably, coumarins bearing alkenyl or alkynyl groups tended to undergo intramolecular [2 + 2] cycloadditions in related radical reactions.⁴⁸ Additionally, an array of coumarins bearing either electron-donating (OMe and Me) or electron-withdrawing (F, Cl, Br, CO₂Me, and NO₂) groups at the *ortho*, *meta*, and *para* positions of the phenyl rings (R²), as well as a polyaromatic naphthalene ring, smoothly participated in the reaction, furnishing the expected BCHs **29–41** in 48–94% yields with 91–97% e.e.

Substrate Scope for BCBs with 2-Pyrone or Chromenes. Encouraged by the above success and the potential of BCHs to expand 3D chemical space for drug discovery, we were naturally eager to extend the methodology to other olefin components to access diverse potentially useful chiral BCHs. Initially, we expected the asymmetric intermolecular [4 π + 2 σ] cycloadditions of BCBs with 2-pyrone to furnish chiral bicyclo[4.1.1]octanes under similar reaction conditions to those used in the well-established catalytic asymmetric Diels–Alder reactions of 2-pyrone with olefins in the presence of an LA and chiral ligand.⁴⁹ Surprisingly, the transformation proceeded well to give the corresponding BCHs **42–46** in 59–85% yields with 90–95% e.e. via the asymmetric [2 π + 2 σ] cycloadditions of BCBs with 2-pyrone (Table 3A). These results greatly expanded the known reaction paradigms of 2-pyrone and opened new avenues for accessing diverse bioactive molecules. Furthermore, it was even more encouraging to note that the asymmetric [2 π + 2 σ] cycloadditions of BCBs with chromenes⁵⁰ also proceeded smoothly, delivering the corresponding BCHs **47–52** in 72–95% yields with 83–95% e.e. under similar reaction conditions (Table 3B). The resulting chiral BCHs contain the core motif of chromanones, which are recognized as privileged structures in flavonoids with a wide

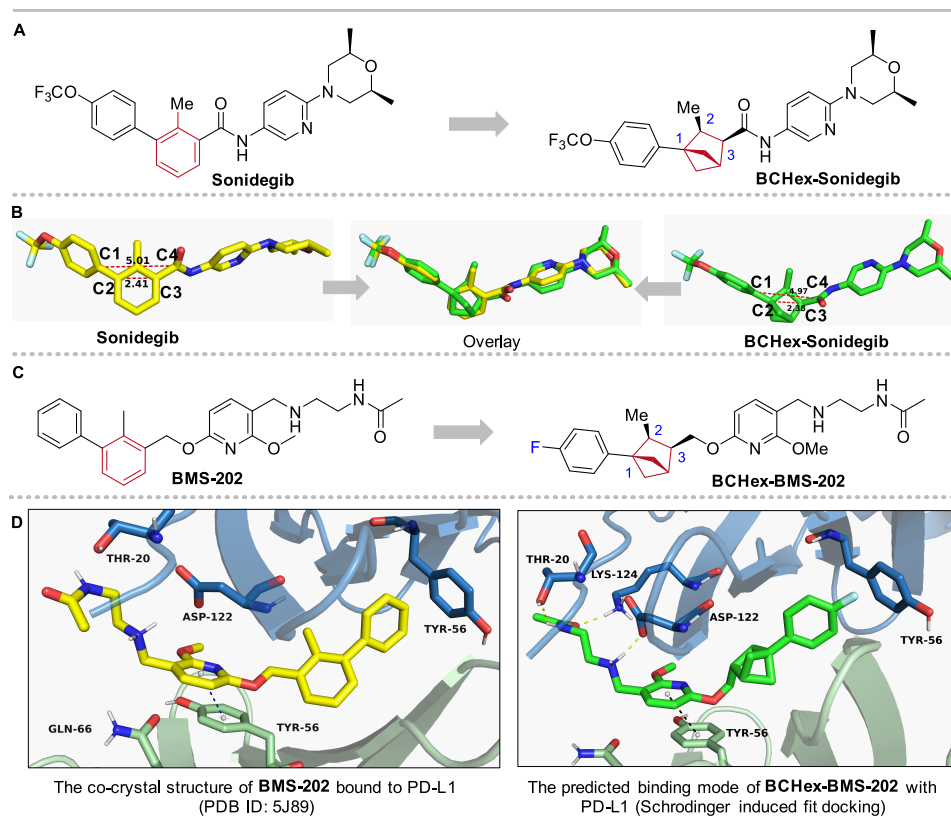
spectrum of bioactivities.⁵¹ The absolute configuration of (*S,S*)-**51** was determined by X-ray crystallographic analysis (Figure S4 in the SI).

Synthetic Utility. To further demonstrate the practicality of the current methodology for bioisosteric replacement, we carried out a gram-scale synthesis of chiral BCH **13** (Scheme 2A). The asymmetric [2 π + 2 σ] cycloaddition of **B11** with **C1** was performed on a 3.36 mmol scale under standard reaction conditions, and 1.58 g of chiral BCH **13** was prepared with high reaction efficiency and excellent enantioselectivity. Next, several synthetic transformations were carried out to highlight the potential applications of BCH **1** (Scheme 2B). Initially, hydrolysis of the acyl pyrazole group of **1** afforded the free carboxylic acid **53**, which was activated by the reaction with NHPI (*N*-hydroxyphthalimide) to furnish the NHPI ester **54**. Subsequently, a photoinduced decarboxylative transformation of **54** delivered the iodide-containing BCH **55**,⁵² providing opportunities for further transformations with diverse nucleophiles. Additionally, the nickel-catalyzed decarboxylative fragmentation of the redox-active ester **54** afforded the 1,2,3-trisubstituted BCH **56** in excellent yield.⁵³ Moreover, a photoinduced decarboxylative borylation of **54** in the presence of the bis(catecholato)diboron (B₂cat₂) and pinacol delivered the Bpin-containing compound **57**,⁵⁴ a synthetically useful building block for downstream functionalizations.⁵⁵ Subsequent oxidation of boronic ester **57** led to the formation of alcohol **58** in high yield. Importantly, there was no noticeable loss of enantiopurity in any of the transformations mentioned above, thereby confirming the practicality of this method in synthetic chemistry. The removal of the exocyclic ester group of **56** in the presence of LiCl afforded **59**. Subsequently, **59** underwent ester hydrolysis, followed by reesterification with MeI to yield **60**, which was recrystallized to enhance enantiopurity. **60** was then successfully oxidized to convert the electron-rich anisole group to a carboxylic acid to deliver the corresponding **61**. The carboxylic acid of **61** was activated by the reaction with NHPI to furnish the NHPI ester **62**. Finally, nickel-catalyzed decarboxylative fragmentation of redox-active **62** afforded the desired 1,2-disubstituted BCH **63** (Scheme 2C).

In the context of drug discovery, different stereoisomers of a drug or biologically active molecule tend to display distinct therapeutic properties or adverse effects.⁵⁶ Consequently, the development of enantioselective strategies that enable highly efficient access to both enantiomers of chiral molecules is highly desirable. The stereodivergent synthesis of molecules containing multistereogenic centers has evolved as a powerful tool for assembling diverse chemical entities in highly enantioenriched forms using both enantiomers of a chiral catalyst. Thus, we set out to establish the stereodivergent access to BCH **12** using *ent*-L***12**. As a result, the enantiomer of BCH **12** was readily obtained in excellent yield with excellent enantio- and diastereoselectivity (Scheme 2D). The absolute configuration of (*R,R*)-**12** was determined by X-ray crystallographic analysis (Figure S5 in the SI).

Bioisosteric Replacement. To demonstrate the potential of BCHs as benzene isosteres in medicinal chemistry, we envisioned that the newly developed methodology could be applied to the synthesis of more complex BCHs of medicinal value. In this context, the incorporation of 1,2- and 1,5-disubstituted BCHs into the antifungal agents such as Boskaldin and Fluxapyroxad, as well as the antimicrobial phthalylsulfathiazole, as saturated bioisosteres of *ortho*-substituted ben-

Scheme 3. Bioisosteric Replacement and Computational Prediction

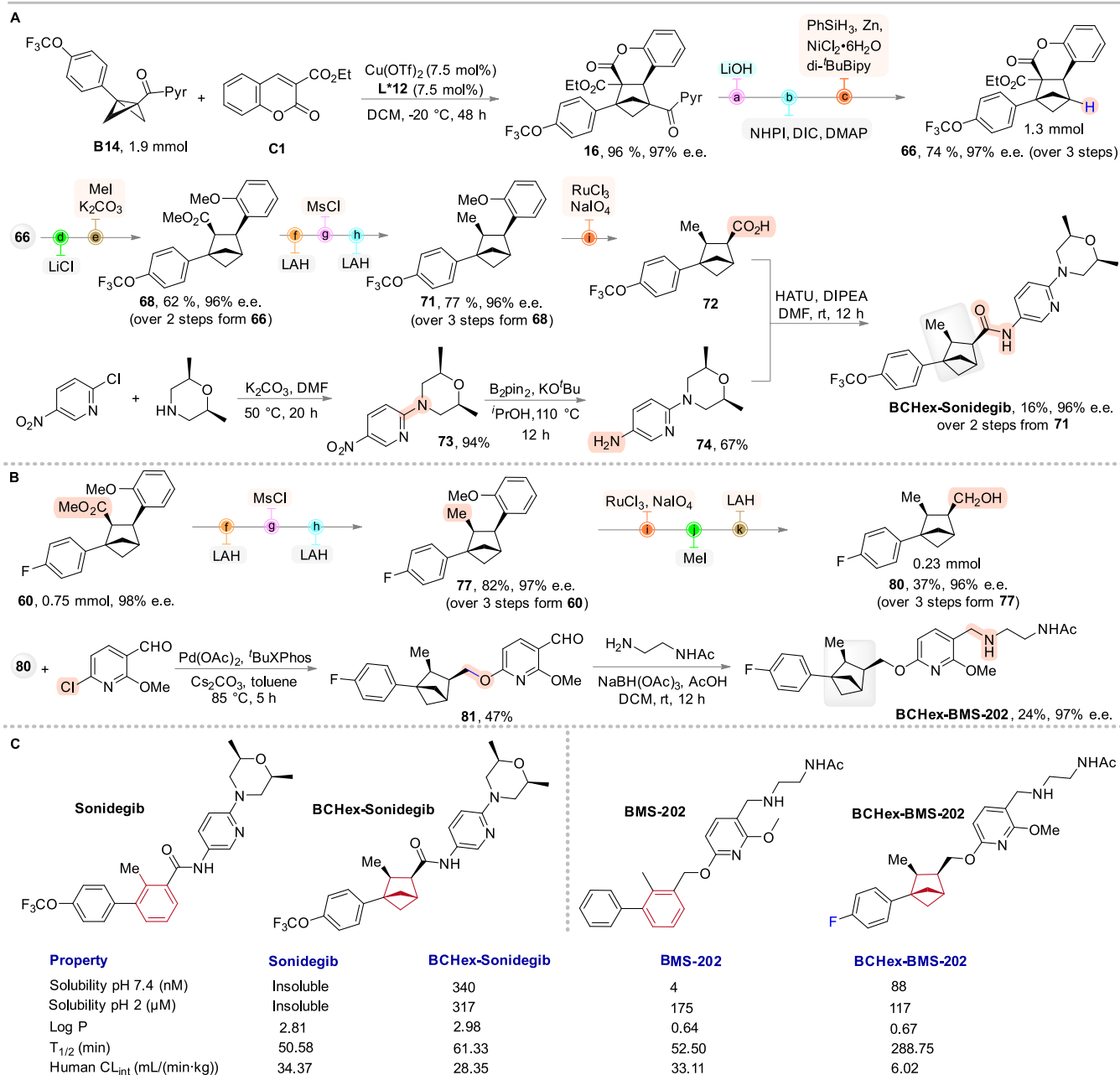


zenes, was successively developed by Mykhailiuk^{6a,25} and Procter.^{6c} However, these approaches were restricted to *ortho*-substituted benzenes. The bioisosteric replacement of other benzene substitution patterns, particularly 1,2,3-trisubstituted benzenes, one of the common scaffolds in active pharmaceutical ingredients¹⁰ with 1,2,3-trisubstituted BCHs bearing two stereogenic centers has not yet been explored.¹⁰ To showcase the value of such 1,2,3-trisubstituted BCHs as a mimic for 1,2,3-trisubstituted benzene, and in alignment with our ongoing commitment to developing antitumor drugs,⁵⁷ chiral BCHex-Sonidegib, an analogue of an anticancer drug Sonidegib,⁴⁰ and chiral BCHex-BMS-202, an analogue of the nonpeptidic PD-1/PD-L1 inhibitor BMS-202,⁴¹ were carefully designed and synthesized, and their antitumor activities were evaluated through biological studies. Starting with computational prediction of their physicochemical properties in medicinal chemistry, the 1,2,3-trisubstituted phenyl group in Sonidegib was replaced with a chiral 1,2,3-trisubstituted BCH, resulting in BCHex-Sonidegib (Scheme 3A). By simulating the 3D conformations of both molecules using Schrodinger software and performing a conformational overlay, we found that the C1–C4 distances were 2.41 and 2.38 Å, respectively, and the C2–C3 distances were 5.01 and 4.97 Å, respectively. Thus, the 3D conformations of both molecules overlapped well, indicating that their spatial geometric features were essentially identical (Scheme 3B). Moreover, the trisubstituted phenyl group in BMS-202 was also replaced with a chiral 1,2,3-trisubstituted BCH to obtain BCHex-BMS-202 (Scheme 3C). We predicted the binding mode of BCHex-BMS-202 with PD-L1 using the induced fit docking (flexible docking) simulation in Schrodinger 2021–2 software (Scheme 3D), and the results indicated that the 3D conformations of both molecules did not

change significantly. Consistent with BMS-202, BCHex-BMS-202 also retained the key π – π stacking between the pyridine ring and the phenyl ring of tyrosine Tyr-56. More importantly, compared to BMS-202, the new formation of multiple hydrogen bonds between the polar chain and the surrounding amino acid residues, including Thr-20, Asp-122, and Lys-124, contributed to enhancing the interaction between BCHex-BMS-202 and the target protein. Additionally, since the 1,2,3-trisubstituted benzene ring in BMS-202 mainly acted as a linker, replacing it with a chiral 1,2,3-trisubstituted BCHs in bioactive compounds exhibited similar spatial geometric features. This highlights the potential use of chiral BCHs as benzene bioisosteres, introducing novel perspectives and approaches for drug design.

Synthesis of Chiral BCHex-Sonidegib and BCHex-BMS-202. The synthetic route from **16** to **68** followed a similar pathway to **60** (Scheme 2). Subsequently, **68** was reduced with lithium aluminum hydride (LAH) to yield **69**, which was then protected with MsCl, and the subsequent reduction with LAH led to the formation of **71**. Next, **71** was successfully oxidized to convert the electron-rich anisole group to a carboxylic acid to yield **72**. The amidation between **72** and **74**^{7a} furnished the target chiral BCHex-Sonidegib, an analogue of Sonidegib with 96% e.e. (Scheme 4A). Furthermore, BCHex-BMS-202 was prepared from **60**, and the key intermediate **80** was synthesized with 96% e.e. over six steps following a similar synthetic protocol used for **72**. Then, **80** underwent a palladium-catalyzed cross-coupling with commercially available 6-chloro-2-methoxynicotinaldehyde to deliver

Scheme 4. Synthesis and Assessment of the Physicochemical Properties of Chiral BCHex-Sonidegib and BCHex-BMS-202



81. Finally, NaBH(OAc)₃-mediated reductive amination of **81** expediently afforded the chiral BCHex-BMS-202, an analogue of BMS-202 with 97% e.e.⁴¹ (Scheme 4B).

Biological Activity of Chiral BCHex-Sonidegib and BCHex-BMS-202. First, the physicochemical and pharmacological properties of chiral BCHex-Sonidegib and BCHex-BMS-202 were assessed in comparison to Sonidegib and BMS-202, respectively (Scheme 4C). Both analogues demonstrated significantly improved solubility at pH 7.4 (simulating conditions in the blood or small intestine) and pH 2 (mimicking the acidic environment of the stomach), indicating that the bioisosteric replacement had the potential to enhance the drugs' bioavailability. Meanwhile, they demonstrated similar lipophilicity (log *P*) to their aryl-containing counterparts. Additionally, chiral BCHex-Sonidegib and BCHex-BMS-202 exhibited lower intrinsic clearance (CL_{int}) in human liver

microsomes (*in vitro* human Clint, mL/(min·kg)), and had longer half-life (T_{1/2}) than Sonidegib and BMS-202, respectively (see the SI for details). These findings indicate that chiral BCHex-Sonidegib and BCHex-BMS-202 are more metabolically stable than their parent compounds, demonstrating the potential of 1,2,3-trisubstituted BCHs for improving the physicochemical and pharmacological properties of drug candidates. Second, the antitumor activities of chiral BCHex-Sonidegib and BCHex-BMS-202 were evaluated against various human cancer cell lines. Sonidegib acts as a Smoothed antagonist to inhibit the Hedgehog signaling pathway in lung⁵⁸ and pancreatic cancers.^{40,58a,59} Meanwhile, these cancer cells⁶⁰ often express PD-L1, a protein targeted by BMS-202 to block the PD-1/PD-L1 interaction.⁶¹ To evaluate their potential therapeutic benefits and safety profiles, we assessed the antitumor activity and hepatotoxicity of BCHex-

Table 4. Antitumor Activities of Compounds against Human Cancer Cell Lines and Normal Hepatocytes^a

| compound | IC ₅₀ (μM) ^a | | | | |
|-----------------|------------------------------------|------------|------------|------------|------------|
| | A549 | NCI-H1975 | PANC-1 | MIA PaCa-2 | MIHA |
| Sonidegib | 4.2 ± 0.4 | 5.2 ± 1.2 | 39.9 ± 3.8 | 19.9 ± 3.5 | 14.2 ± 1.0 |
| BCHex-sonidegib | 11.8 ± 0.7 | 18.9 ± 2.3 | 26.2 ± 2.6 | 18.7 ± 2.2 | 21.5 ± 2.3 |
| BMS-202 | 3.7 ± 0.2 | 4.4 ± 0.3 | 6.2 ± 1.6 | 3.9 ± 0.1 | 3.6 ± 1.0 |
| BCHex-BMS-202 | 4.5 ± 0.1 | 5.3 ± 0.6 | 8.5 ± 2.0 | 4.1 ± 0.3 | 3.9 ± 0.9 |

^aData are expressed as the mean ± SD (standard deviation) from the dose–response curves of three independent experiments for 72 h.

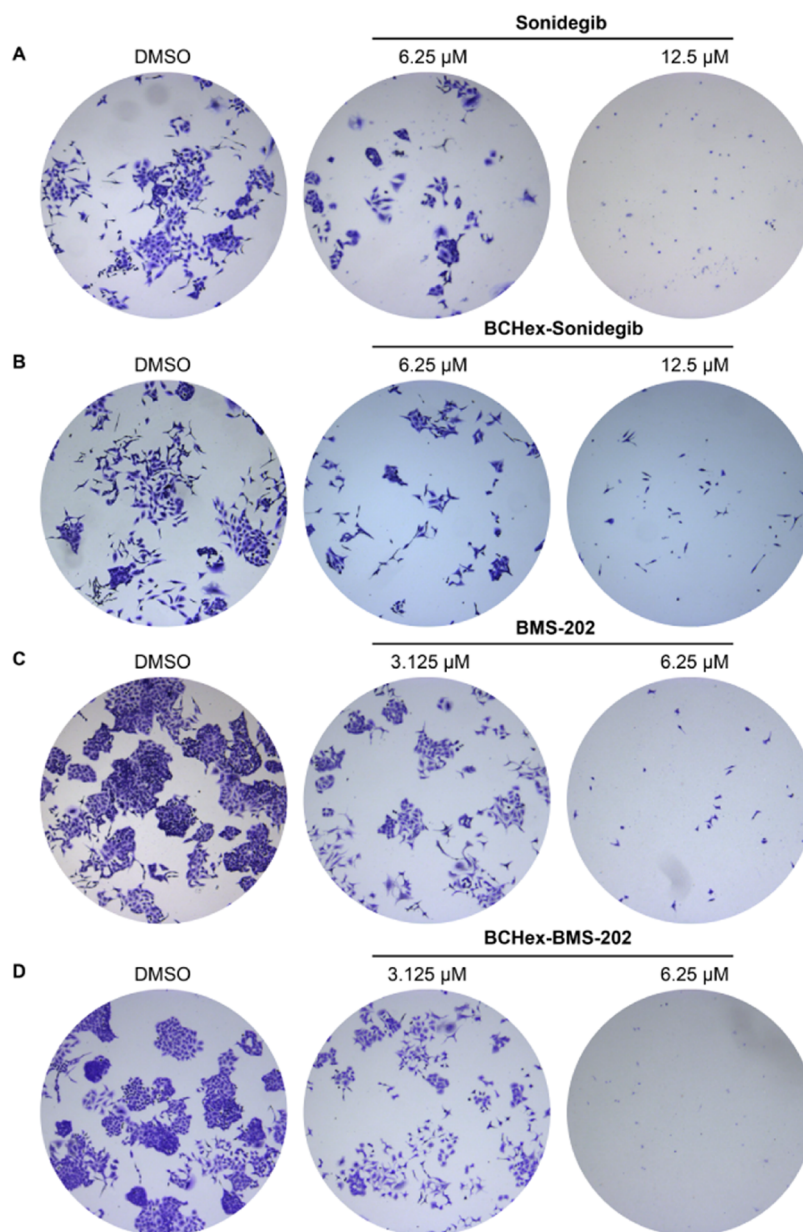
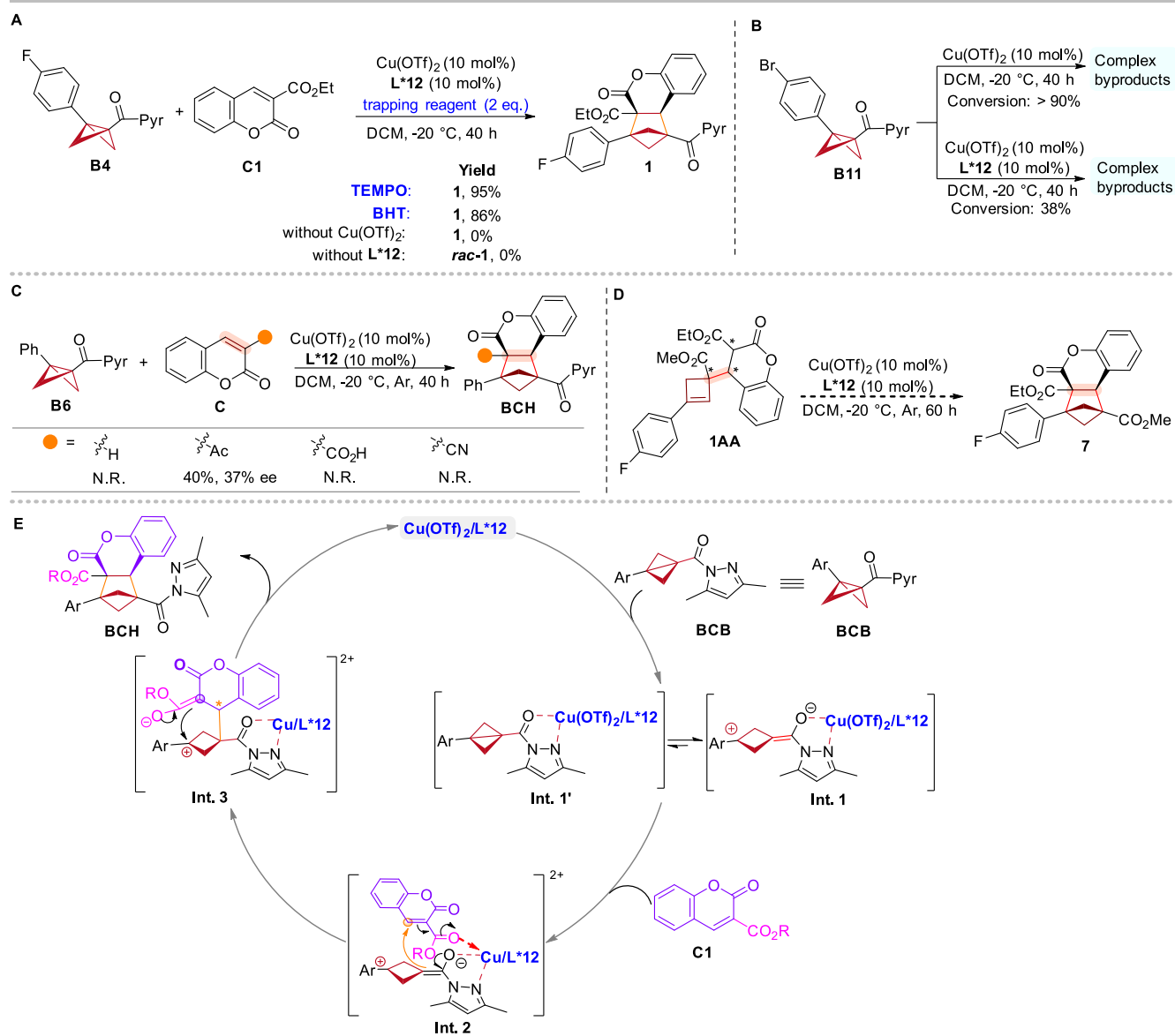


Figure 1. Colony formation assay of A549 cells treated with Sonidegib, BCHex-Sonidegib, BMS-202, and BCHex-BMS-202 for 5 days, respectively.

Sonidegib and BCHex-BMS-202 across several cell lines, including A549, NCI-H1975, PANC-1, MIA PaCa-2, and MIHA (Table 4, MTT assay method, see the SI for details), using Sonidegib and BMS-202 as positive control drugs, respectively. The results revealed that BCHex-Sonidegib demonstrated lower antitumor activity in lung cancer cell lines compared to Sonidegib. However, it exhibited enhanced activity in pancreatic cancer cell lines and reduced

hepatocellular toxicity, suggesting its potential selectivity for different tumor cell types and lower toxicity. Meanwhile, BCHex-BMS-202 exhibited antitumor activity and hepatocellular toxicity comparable to that of BMS-202. Furthermore, we also assessed the antiproliferative effects of these four compounds on A549 using colony formation assays (Figure 1, see the SI for details). All compounds displayed significant dose-dependent antiproliferative activity. Sonidegib and

Scheme 5. Mechanistic Experiments and Proposed Mechanism



BCHex-Sonidegib almost completely inhibited colony formation at 12.5 μM , whereas BMS-202 and BCHex-BMS-202 achieved similar effects at a lower concentration of 6.25 μM . Finally, flow cytometry analysis revealed that these four compounds could induce apoptosis in A549 cells (Figure S10 in the SI). Altogether, these results further supported the promising application of chiral BCHs as bioisosteres for phenyl rings, offering fresh insights and strategies for drug design in medicinal chemistry.

Mechanistic Studies. To obtain insight into the reaction mechanism, a series of control experiments were conducted. Initially, the current cycloaddition was not completely inhibited by the addition of 2.0 equiv of TEMPO (2,2,6,6-tetramethyl-1-piperidinyloxy) or 2.0 equiv of BHT (butylated hydroxytoluene) as radical trapping reagents. Additionally, none of the corresponding radical trapping products were detected by ¹H NMR or HRMS (high-resolution mass spectroscopy), suggesting that a radical process might not be involved in the reaction (Scheme 5A). Furthermore, no desired BCH 1 was observed in the absence of the LA or chiral ligand.

These observations, together with the above-mentioned significant effects of different chiral ligands in the reaction condition optimization study (Table 1), indicated that both the LA and chiral ligand are essential for this transformation. To gain deeper insight into the essential roles of the chiral ligand, we treated B11 with the LA alone or both the LA and chiral ligand. The reaction with the LA alone furnished several unidentified byproducts, indicating that BCB was easily decomposed in the presence of the LA,³⁷ as detected by ¹H NMR. However, the addition of a chiral ligand greatly inhibited this process, revealing that the chiral ligand could effectively diminish the acidity of the LA to suppress the decomposition of BCBs, consistent with the previous reports³⁷ (Scheme 5B). To further understand the key role of the exocyclic ester group of coumarin C1 for the transformation, other coumarin substrates bearing acetyl, carboxyl, and cyano groups were tested under identical conditions. These substrates hardly led to the desired products at -20 °C. Only the coumarin bearing an acetyl group gave an unsatisfactory result, indicating that the exocyclic ester group

of coumarin was essential for this reaction. This ester group potentially functioned as a coordinating group to bind with LA, thereby facilitating both reactivity and stereoselection (Scheme 5C). Finally, to exclude the possibility of BCH formation via the intermediacy of cyclobutenyl oxochromane, 1AA was subjected to standard conditions. Nevertheless, the desired BCH 7 was not observed, revealing that the cycloadditions of BCBs did not proceed via the cyclobutenyl oxochromane intermediate (Scheme 5D).

Based on the above observations and previous reports,^{33a,37,45,62} a possible reaction mechanism for the LA-catalyzed asymmetric intermolecular $[2\pi + 2\sigma]$ cycloaddition of BCBs was proposed (Scheme 5E). Initially, the Cu(II)/Box complex coordinates with the acyl pyrazole group of BCBs to activate them, followed by ring-opening to generate the enolate species **Int. 1** via tautomerization. Subsequently, the resulting complex reacts with coumarin **C1** to furnish the key **Int. 2**, where Cu(II) coordinates with both the exocyclic carbonyl group⁵⁰ of coumarin **C1** and the acyl pyrazole group⁴⁵ of the BCBs for reactivity and stereoselection. The enolate then undergoes a Michael addition to the α,β -unsaturated C=C of coumarin **C1** to generate **Int. 3**, of which the following intramolecular cyclization affords the final BCH product.

CONCLUSIONS

In summary, we have demonstrated the LA-catalyzed asymmetric intermolecular $[2\pi + 2\sigma]$ cycloadditions of BCBs with coumarins, 2-pyrone, or chromenes, facilitating the efficient generation of a variety of sought-after enantioenriched 1,2,3,4-tetrasubstituted BCHs bearing vicinal tertiary-quaternary stereocenters. Key to the success is the use of chiral Box ligands to effectively diminish the acidity of the LA to suppress the competitive side reactions, inhibit significant racemic background reactions, and fine-tune the reactivity and regio-, enantio-, and diastereoselectivities of the transformation. This robust and straightforward approach offers several advantages, including mild reaction conditions, good functional group tolerance, and the stereodivergent synthesis of chiral BCHs. It could be scaled up to a gram scale for the synthesis of enantioenriched, highly substituted BCHs. The novel enantioenriched 1,2,3,4-tetrasubstituted 3D frameworks offer a powerful and distinctive tool for exploring novel diverse 3D chemical space in drug discovery. Additionally, subsequent transformations of the resulting BCHs lead to enantioenriched 1,2-di- or 1,2,3-trisubstituted BCHs, which are valuable for bioisosteric replacement. Furthermore, chiral BCHex-Sonidegib and BCHex-BMS-202 were designed and prepared via multistep processes as analogues of the anticancer drug Sonidegib and the nonpeptidic small-molecule PD-1/PD-L1 inhibitor BMS-202, respectively. It was noteworthy that the chiral 1-phenyl-2,3-disubstituted BCH moiety effectively emulated the biphenyl motif of Sonidegib and BMS-202. The bioisosteric replacement improved the physicochemical properties of these drug candidates. Meanwhile, chiral BCHex-Sonidegib and BCHex-BMS-202 demonstrated comparable antitumor activity to their aryl-containing counterparts, exhibiting antiproliferative effects and inducing apoptosis in cancer cells. These findings highlight the potential application of chiral, highly substituted BCHs as benzene bioisosteres in medicinal chemistry. The use of chiral highly substituted BCH motifs could also extend beyond medicinal chemistry and be applied to material sciences in the future.⁶³ Further studies are ongoing to design and synthesize more bioactive molecules

bearing the chiral BCH motif for medicinal chemistry research in our lab.

ASSOCIATED CONTENT

Supporting Information

The Supporting Information is available free of charge at <https://pubs.acs.org/doi/10.1021/jacs.4c10968>.

Experimental procedures; characterization of compounds; reaction condition optimization with BCB **B1** and ethyl coumarin-3-carboxylate **C1**; screening of different ligands; chiral saturated bicyclic hydrocarbon bioisosteres available for *ortho*-,*meta*-disubstituted and 1,2,3-trisubstituted benzenes; X-ray structure of **12**; and crystallographic data of **12**, *ent*-**12**, and **51** (PDF)

Accession Codes

Deposition Numbers 2371764, 2371766, and 2371784 contain the supplementary crystallographic data for this paper. These data can be obtained free of charge via the joint Cambridge Crystallographic Data Centre (CCDC) and Fachinformationszentrum Karlsruhe [Access Structures](#) service.

AUTHOR INFORMATION

Corresponding Authors

Yuyang Jiang – State Key Laboratory of Chemical Oncogenomics, Institute of Biopharmaceutics and Health Engineering, Tsinghua Shenzhen International Graduate School, Shenzhen 518055, China; Institute of Biomedical Health Technology and Engineering, Shenzhen Bay Laboratory, Shenzhen 518132, China; orcid.org/0000-0003-3904-4855; Email: jiangyy@sz.tsinghua.edu.cn

Xin-Yuan Liu – Shenzhen Grubbs Institute, Department of Chemistry, and Guangming Advanced Research Institute, Southern University of Science and Technology, Shenzhen 518055, China; orcid.org/0000-0002-6978-6465; Email: liuxy3@sustech.edu.cn

Jin-Shun Lin – State Key Laboratory of Chemical Oncogenomics, Institute of Biopharmaceutics and Health Engineering, Tsinghua Shenzhen International Graduate School, Shenzhen 518055, China; orcid.org/0000-0002-4528-7266; Email: lin.jinshun@sz.tsinghua.edu.cn

Authors

Ying-Jie Li – State Key Laboratory of Chemical Oncogenomics, Institute of Biopharmaceutics and Health Engineering, Tsinghua Shenzhen International Graduate School, Shenzhen 518055, China

Zhi-Long Wu – State Key Laboratory of Chemical Oncogenomics, Institute of Biopharmaceutics and Health Engineering, Tsinghua Shenzhen International Graduate School, Shenzhen 518055, China

Qiang-Shuai Gu – Shenzhen Grubbs Institute, Department of Chemistry, and Guangming Advanced Research Institute, Southern University of Science and Technology, Shenzhen 518055, China; orcid.org/0000-0002-3840-425X

Tingting Fan – Institute of Biomedical Health Technology and Engineering, Shenzhen Bay Laboratory, Shenzhen 518132, China

Ming-Hao Duan – State Key Laboratory of Chemical Oncogenomics, Institute of Biopharmaceutics and Health Engineering, Tsinghua Shenzhen International Graduate School, Shenzhen 518055, China

Lihong Wu – State Key Laboratory of Chemical Oncogenomics, Institute of Biopharmaceutics and Health Engineering, Tsinghua Shenzhen International Graduate School, Shenzhen 518055, China

Yu-Tao Wang – State Key Laboratory of Chemical Oncogenomics, Institute of Biopharmaceutics and Health Engineering, Tsinghua Shenzhen International Graduate School, Shenzhen 518055, China

Ji-Peng Wu – State Key Laboratory of Chemical Oncogenomics, Institute of Biopharmaceutics and Health Engineering, Tsinghua Shenzhen International Graduate School, Shenzhen 518055, China

Fang-Lei Fu – State Key Laboratory of Chemical Oncogenomics, Institute of Biopharmaceutics and Health Engineering, Tsinghua Shenzhen International Graduate School, Shenzhen 518055, China

Fan Sang – Institute of Biomedical Health Technology and Engineering, Shenzhen Bay Laboratory, Shenzhen 518132, China

Ai-Ting Peng – State Key Laboratory of Chemical Oncogenomics, Institute of Biopharmaceutics and Health Engineering, Tsinghua Shenzhen International Graduate School, Shenzhen 518055, China

Complete contact information is available at:

<https://pubs.acs.org/10.1021/jacs.4c10968>

Author Contributions

[†]Y.-J.L., Z.-L.W., Q.-S.G., and T.F. contributed equally to this work. The manuscript was written with contributions from all authors. These authors contributed equally.

Notes

The authors declare no competing financial interest.

ACKNOWLEDGMENTS

Financial support from the Shenzhen Science and Technology Innovation Commission (Nos. 2021293, 202231, and KQTD20210811090112004), Guangdong Innovative Program (2019BT02Y335), and the Startup Fund from Shenzhen Bay Laboratory (No. 21310051) is gratefully acknowledged. The authors highly appreciate the help with the photocatalytic reactions provided by Prof. Wujiong Xia, Prof. Lin Guo, and Dr. Chengcheng Shi from the State Key Lab of Urban Water Resource and Environment, School of Science, Harbin Institute of Technology (Shenzhen), as well as the assistance with X-ray crystallographic analysis provided by Dr. Xiao-Yong Chang from the Department of Chemistry, SUSTech.

REFERENCES

- (1) (a) Lovering, F.; Bikker, J.; Humblet, C. Escape from Flatland: Increasing Saturation as an Approach to Improving Clinical Success. *J. Med. Chem.* **2009**, *52*, 6752–6756. (b) Lovering, F. Escape from Flatland 2: Complexity and Promiscuity. *Med. Chem. Commun.* **2013**, *4*, 515–519.
- (2) Wei, W.; Cherukupalli, S.; Jing, L.; Liu, X.; Zhan, P. Fsp³: A New Parameter for Drug-likeness. *Drug Discovery Today* **2020**, *25*, 1839–1845.
- (3) Méndez-Lucio, O.; Medina-Franco, J. L. The Many Roles of Molecular Complexity in Drug Discovery. *Drug Discovery Today* **2017**, *22*, 120–126.
- (4) Tsien, J.; Hu, C.; Merchant, R. R.; Qin, T. Three-dimensional Saturated C(sp³)-rich Bioisosteres for Benzene. *Nat. Rev. Chem.* **2024**, *8*, 605–627.

- (5) (a) Stepan, A. F.; Subramanyam, C.; Efremov, I. V.; Dutra, J. K.; O'Sullivan, T. J.; DiRico, K. J.; McDonald, W. S.; Won, A.; Dorff, P. H.; Nolan, C. E.; Becker, S. L.; Pustilnik, L. R.; Riddell, D. R.; Kauffman, G. W.; Kormos, B. L.; Zhang, L.; Lu, Y.; Capetta, S. H.; Green, M. E.; Karki, K.; Sibley, E.; Atchison, K. P.; Hallgren, A. J.; Oborski, C. E.; Robshaw, A. E.; Sneed, B.; O'Donnell, C. J. Application of the Bicyclo[1.1.1]pentane Motif as a Nonclassical Phenyl Ring Bioisostere in the Design of a Potent and Orally Active Gamma-secretase Inhibitor. *J. Med. Chem.* **2012**, *55*, 3414–3424. (b) Gianatassio, R.; Lopchuk, J. M.; Wang, J.; Pan, C.-M.; Malins, L. R.; Prieto, L.; Brandt, T. A.; Collins, M. R.; Gallego, G. M.; Sach, N. W.; Spangler, J. E.; Zhu, H.; Zhu, J.; Baran, P. S. Strain-Release Amination. *Science* **2016**, *351*, 241–246.
- (6) (a) Denisenko, A.; Garbuz, P.; Shishkina, S. V.; Voloshchuk, N. M.; Mykhailiuk, P. K. Saturated Bioisosteres of *ortho*-Substituted Benzenes. *Angew. Chem., Int. Ed.* **2020**, *59*, 20515–20521. (b) Kleinmans, R.; Pinkert, T.; Dutta, S.; Paulisch, T. O.; Keum, H.; Daniliuc, C. G.; Glorius, F. Intermolecular [2 π +2 σ]-Photocycloaddition Enabled by Triplet Energy Transfer. *Nature* **2022**, *605*, 477–482. (c) Agasti, S.; Beltran, F.; Pye, E.; Kaltsoyannis, N.; Crisenza, G. E. M.; Procter, D. J. A Catalytic Alkene Insertion Approach to Bicyclo[2.1.1]hexane Bioisosteres. *Nat. Chem.* **2023**, *15*, 535–541.
- (7) (a) Frank, N.; Nugent, J.; Shire, B. R.; Pickford, H. D.; Rabe, P.; Sterling, A. J.; Zarganes-Tzitzikas, T.; Grimes, T.; Thompson, A. L.; Smith, R. C.; Schofield, C. J.; Brennan, P. E.; Duarte, F.; Anderson, E. A. Synthesis of *meta*-Substituted Arene Bioisosteres from [3.1.1]-Propellane. *Nature* **2022**, *611*, 721–726. (b) Nguyen, T. V. T.; Bossonnet, A.; Wodrich, M. D.; Waser, J. P. Photocatalyzed [2 σ + 2 σ] and [2 π + 2 σ] Cycloadditions for the Synthesis of Bicyclo[3.1.1]-heptanes and 5- or 6-Membered Carbocycles. *J. Am. Chem. Soc.* **2023**, *145*, 25411–25421. (c) Yu, T.; Yang, J.; Wang, Z.; Ding, Z.; Xu, M.; Wen, J.; Xu, L.; Li, P. Selective [2 σ + 2 σ] Cycloaddition Enabled by Boronyl Radical Catalysis: Synthesis of Highly Substituted Bicyclo[3.1.1]heptanes. *J. Am. Chem. Soc.* **2023**, *145*, 4304–4310.
- (8) (a) Reekie, T. A.; Williams, C. M.; Rendina, L. M.; Kassiou, M. Cubanes in Medicinal Chemistry. *J. Med. Chem.* **2019**, *62*, 1078–1095. (b) Wiesenfeldt, M. P.; Rossi-Ashton, J. A.; Perry, I. B.; Diesel, J.; Garry, O. L.; Bartels, F.; Coote, S. C.; Ma, X.; Yeung, C. S.; Bennett, D. J.; MacMillan, D. W. C. General Access to Cubanes as Benzene Bioisosteres. *Nature* **2023**, *618*, 513–518.
- (9) Subbaiah, M. A. M.; Meanwell, N. A. Bioisosteres of the Phenyl Ring: Recent Strategic Applications in Lead Optimization and Drug Design. *J. Med. Chem.* **2021**, *64*, 14046–14128.
- (10) Nilova, A.; Campeau, L.-C.; Sherer, E. C.; Stuart, D. R. Analysis of Benzenoid Substitution Patterns in Small Molecule Active Pharmaceutical Ingredients. *J. Med. Chem.* **2020**, *63*, 13389–13396.
- (11) Talele, T. T. Opportunities for Tapping into Three-dimensional Chemical Space through a Quaternary Carbon. *J. Med. Chem.* **2020**, *63*, 13291–13315.
- (12) (a) Golfmann, M.; Walker, J. C. L. Bicyclobutanes as Unusual Building Blocks for Complexity Generation in Organic Synthesis. *Commun. Chem.* **2023**, *6*, No. 9. (b) Sujansky, S. J.; Ma, X. Reaction Paradigms that Leverage Cycloaddition and Ring Strain to Construct Bicyclic Aryl Bioisosteres from Bicyclo[1.1.0]butanes. *Asian J. Org. Chem.* **2024**, *13*, No. e202400045.
- (13) Paul, S.; Adelfinsky, D.; Salome, C.; Fessard, T.; Brown, M. K. 2,5-Disubstituted Bicyclo[2.1.1]hexanes as Rigidified Cyclopentane Variants. *Chem. Sci.* **2023**, *14*, 8070–8075.
- (14) Wipf, P.; Walczak, M. A. Pericyclic Cascade Reactions of (Bicyclo[1.1.0]butylmethyl)amines. *Angew. Chem., Int. Ed.* **2006**, *45*, 4172–4175.
- (15) Dutta, S.; Lee, D.; Ozols, K.; Daniliuc, C. G.; Shintani, R.; Glorius, F. Photoredox-Enabled Dearomative [2 π + 2 σ] Cycloaddition of phenols. *J. Am. Chem. Soc.* **2024**, *146*, 2789–2797.
- (16) Kleinmans, R.; Dutta, S.; Ozols, K.; Shao, H.; Schafer, F.; Thielemann, R. E.; Chan, H. T.; Daniliuc, C. G.; Houk, K. N.; Glorius, F. *ortho*-Selective Dearomative [2 π + 2 σ] Photocycloadditions of Bicyclic Aza-arenes. *J. Am. Chem. Soc.* **2023**, *145*, 12324–12332.

- (17) Liu, Y.; Wu, Z.; Shan, J.-R.; Yan, H.; Hao, E.-J.; Shi, L. Titanium Catalyzed $[2\pi + 2\sigma]$ Cycloaddition of Bicyclo[1.1.0]butanes with 1,3-Dienes for Efficient Synthesis of Stilbene Bioisosteres. *Nat. Commun.* **2024**, *15*, No. 4374.
- (18) Tyler, J. L.; Schäfer, F.; Shao, H.; Stein, C.; Wong, A.; Daniliuc, C. G.; Houk, K. N.; Glorius, F. Bicyclo[1.1.0]butyl Radical Cations: Synthesis and Application to $[2\pi + 2\sigma]$ Cycloaddition Reactions. *J. Am. Chem. Soc.* **2024**, *146*, 16237–16247.
- (19) Guo, R.; Chang, Y.-C.; Herter, L.; Salome, C.; Braley, S. E.; Fessard, T. C.; Brown, M. K. Strain-Release $[2\pi + 2\sigma]$ Cycloadditions for the Synthesis of Bicyclo[2.1.1]hexanes Initiated by Energy Transfer. *J. Am. Chem. Soc.* **2022**, *144*, 7988–7994.
- (20) Xu, M.; Wang, Z.; Sun, Z.; Ouyang, Y.; Ding, Z.; Yu, T.; Xu, L.; Li, P. Diboron(4)-Catalyzed Remote $[3 + 2]$ Cycloaddition of Cyclopropanes via Dearomative/Rearomative Radical Transmission through Pyridine. *Angew. Chem., Int. Ed.* **2022**, *61*, No. e202214507.
- (21) Liu, Y.; Lin, S.; Li, Y.; Xue, J.-H.; Li, Q.; Wang, H. Pyridine-Boryl Radical-Catalyzed $[2\pi + 2\sigma]$ Cycloaddition of Bicyclo[1.1.0]butanes with Alkenes. *ACS Catal.* **2023**, *13*, 5096–5103.
- (22) Radhoff, N.; Daniliuc, C. G.; Studer, A. Lewis Acid Catalyzed Formal $(3 + 2)$ -Cycloaddition of Bicyclo[1.1.0]butanes with Ketenes. *Angew. Chem., Int. Ed.* **2023**, *62*, No. e202304771.
- (23) Ni, D.; Hu, S.; Tan, X.; Yu, Y.; Li, Z.; Deng, L. Intermolecular Formal Cycloaddition of Indoles with Bicyclo[1.1.0]butanes by Lewis Acid Catalysis. *Angew. Chem., Int. Ed.* **2023**, *62*, No. e202308606.
- (24) Tang, L.; Xiao, Y.; Wu, F.; Zhou, J.-L.; Xu, T.-T.; Feng, J.-J. Silver-Catalyzed Dearomative $[2\pi + 2\sigma]$ Cycloadditions of Indoles with Bicyclobutanes: Access to Indoline Fused Bicyclo[2.1.1]hexanes. *Angew. Chem., Int. Ed.* **2023**, *62*, No. e202310066.
- (25) Denisenko, A.; Garbuz, P.; Makovetska, Y.; Shablykin, O.; Lesyk, D.; Al-Maali, G.; Korzh, R.; Sadkova, I. V.; Mykhailiuk, P. K. 1,2-Disubstituted Bicyclo[2.1.1]hexanes as Saturated Bioisosteres of ortho-Substituted Benzene. *Chem. Sci.* **2023**, *14*, 14092–14099.
- (26) Reinhold, M.; Steinebach, J.; Golz, C.; Walker, J. C. L. Synthesis of Polysubstituted Bicyclo[2.1.1]hexanes Enabling Access to New Chemical Space. *Chem. Sci.* **2023**, *14*, 9885–9891.
- (27) Posz, J. M.; Sharma, N.; Royalty, P. A.; Liu, Y.; Salome, C.; Fessard, T. C.; Brown, M. K. Synthesis of Borylated Carbocycles by $[2 + 2]$ -Cycloadditions and Photo-Ene Reactions. *J. Am. Chem. Soc.* **2024**, *146*, 10142–10149.
- (28) de Robichon, M.; Kratz, T.; Beyer, F.; Zuber, J.; Merten, C.; Bach, T. Enantioselective, Intermolecular $[\pi_2 + \pi_2]$ Photocycloaddition Reactions of 2(1H)-Quinolones and Bicyclo[1.1.0]butanes. *J. Am. Chem. Soc.* **2023**, *145*, 24466–24470.
- (29) Fu, Q.; Cao, S.; Wang, J.; Lv, X.; Wang, H.; Zhao, X.; Jiang, Z. Enantioselective $[2\pi + 2\sigma]$ Cycloadditions of Bicyclo[1.1.0]butanes with Vinylazaarenes through Asymmetric Photoredox Catalysis. *J. Am. Chem. Soc.* **2024**, *146*, 8372–8380.
- (30) Zhou, J.-L.; Xiao, Y.; He, L.; Gao, X.-Y.; Yang, X.-C.; Wu, W.-B.; Wang, G.; Zhang, J.; Feng, J.-J. Palladium-Catalyzed Ligand-Controlled Switchable Hetero-(5 + 3)/Enantioselective $[2\sigma + 2\sigma]$ Cycloadditions of Bicyclobutanes with Vinyl Oxiranes. *J. Am. Chem. Soc.* **2024**, *146*, 19621–19628.
- (31) Xiao, Y.; Wu, F.; Tang, L.; Zhang, X.; Wei, M.; Wang, G.; Feng, J.-J. Divergent Synthesis of Sulfur-Containing Bridged Cyclobutanes by Lewis Acid Catalyzed Formal Cycloadditions of Pyridinium 1,4-Zwitterionic Thiolates and Bicyclobutanes. *Angew. Chem., Int. Ed.* **2024**, *63*, No. e202408578.
- (32) Wang, X.; Gao, R.; Li, X. Catalytic Asymmetric Construction of Chiral Polysubstituted 3-Azabicyclo[3.1.1]heptanes by Copper-Catalyzed Stereoselective Formal $[4\pi + 2\sigma]$ Cycloaddition. *J. Am. Chem. Soc.* **2024**, *146*, 21069–21077.
- (33) (a) Zhang, X.-G.; Zhou, Z.-Y.; Li, J.-X.; Chen, J.-J.; Zhou, Q.-L. Copper-Catalyzed Enantioselective $[4\pi + 2\sigma]$ Cycloaddition of Bicyclobutanes with Nitrones. *J. Am. Chem. Soc.* **2024**, *146*, 27274–27281. (b) Wu, W.-B.; Xu, B.; Yang, X.-C.; Wu, F.; He, H.-X.; Zhang, X.; Feng, J.-J. Enantioselective Formal (3 + 3) Cycloaddition of Bicyclobutanes with Nitrones Enabled by Asymmetric Lewis Acid Catalysis. *Nat. Commun.* **2024**, *15*, No. 8005.
- (34) Yang, X.-C.; Wu, F.; Wu, W.-B.; Zhang, X.; Feng, J.-J. Enantioselective Dearomatizing Formal (3 + 3) Cycloadditions of Bicyclobutanes with Aromatic Azomethine Imines: Access to Fused 2,3-Diazabicyclo[3.1.1]heptanes. *ChemRxiv* **2024**; Vol. 63 DOI: 10.26434/chemrxiv-2024-zgffb.
- (35) Bai, D.; Guo, X.; Wang, X.; Xu, W.; Cheng, R.; Wei, D.; Lan, Y.; Chang, J. Umpolung Reactivity of Strained C–C σ -Bonds without Transition-Metal Catalysis. *Nat. Commun.* **2024**, *15*, No. 2833.
- (36) (a) Guin, A.; Bhattacharjee, S.; Harariya, M. S.; Biju, A. T. Lewis Acid-Catalyzed Diastereoselective Carbofunctionalization of Bicyclobutanes Employing Naphthols. *Chem. Sci.* **2023**, *14*, 6585–6591. (b) Tang, L.; Huang, Q.-N.; Wu, F.; Xiao, Y.; Zhou, J.-L.; Xu, T.-T.; Wu, W.-B.; Qu, S.; Feng, J.-J. C(sp²)-H Cyclobutylolation of Hydroxyarenes Enabled by Silver- π -Acid Catalysis: Diastereocontrolled Synthesis of 1,3-Difunctionalized Cyclobutanes. *Chem. Sci.* **2023**, *14*, 9696–9703.
- (37) Dhake, K.; Woelk, K. J.; Becica, J.; Un, A.; Jenny, S. E.; Leitch, D. C. Beyond Bioisosteres: Divergent Synthesis of Azabicyclohexanes and Cyclobutenyl Amines from Bicyclobutanes. *Angew. Chem., Int. Ed.* **2022**, *61*, No. e202204719.
- (38) (a) Quasdorf, K. W.; Overman, L. E. Catalytic Enantioselective Synthesis of Quaternary Carbon Stereocentres. *Nature* **2014**, *516*, 181–191. (b) Zhou, F.; Zhu, L.; Pan, B. W.; Shi, Y.; Liu, Y. L.; Zhou, J. Catalytic Enantioselective Construction of Vicinal Quaternary Carbon Stereocenters. *Chem. Sci.* **2020**, *11*, 9341–9365.
- (39) (a) Lin, J.-S.; Dong, X.-Y.; Li, T.-T.; Jiang, N.-C.; Tan, B.; Liu, X.-Y. A Dual-Catalytic Strategy to Direct Asymmetric Radical Aminotrifluoromethylation of Alkenes. *J. Am. Chem. Soc.* **2016**, *138*, 9357–9360. (b) Lin, J.-S.; Li, T.-T.; Liu, J.-R.; Jiao, G.-Y.; Gu, Q.-S.; Cheng, J.-T.; Guo, Y.-L.; Hong, X.; Liu, X.-Y. Cu/Chiral Phosphoric Acid-Catalyzed Asymmetric Three-component Radical-initiated 1,2-Dicarbonylfunctionalization of Alkenes. *J. Am. Chem. Soc.* **2019**, *141*, 1074–1083. (c) Dong, X.-Y.; Zhang, Y.-F.; Ma, C.-L.; Gu, Q.-S.; Wang, F.-L.; Li, Z.-L.; Jiang, S.-P.; Liu, X.-Y. A General Asymmetric Copper-catalyzed Sonogashira C(sp³)-C(sp) Coupling. *Nat. Chem.* **2019**, *11*, 1158–1166. (d) Gu, Q.-S.; Li, Z.-L.; Liu, X.-Y. Copper(I)-Catalyzed Asymmetric Reactions Involving Radicals. *Acc. Chem. Res.* **2020**, *53*, 170–181. (e) Chen, J.-J.; Fang, J.-H.; Du, X.-Y.; Zhang, J.-Y.; Bian, J.-Q.; Wang, C.; Wang, F.-L.; Luan, C.; Liu, W.-L.; Liu, J.-R.; Dong, X.-Y.; Li, Z.-L.; Gu, Q.-S.; Dong, Z.; Liu, X.-Y. Enantioconvergent Cu-Catalyzed N-alkylation of Aliphatic Amines. *Nature* **2023**, *618*, 294–300.
- (40) Casey, D.; Demko, S.; Shord, S.; Zhao, H.; Chen, H.; He, K.; Putman, A.; Helms, W.; Keegan, P.; Pazdur, R. FDA Approval Summary: Sonidegib for Locally Advanced Basal Cell Carcinoma. *Clin. Cancer Res.* **2017**, *23*, 2377–2381.
- (41) Guzik, K.; Zak, K. M.; Grudnik, P.; Magiera, K.; Musielak, B.; Törner, R.; Skalniak, L.; Dömling, A.; Dubin, G.; Holak, T. A. Small-Molecule Inhibitors of the Programmed Cell Death-1/Programmed Death-ligand 1 (PD-1/PD-L1) Interaction via Transiently Induced Protein States and Dimerization of PD-L1. *J. Med. Chem.* **2017**, *60*, 5857–5867.
- (42) Wang, F.-L.; Yang, C.-J.; Liu, J.-R.; Yang, N.-Y.; Dong, X.-Y.; Jiang, R.-Q.; Chang, X.-Y.; Li, Z.-L.; Xu, G.-X.; Yuan, D.-L.; Zhang, Y.-S.; Gu, Q.-S.; Hong, X.; Liu, X.-Y. Mechanism-Based Ligand Design for Copper-catalyzed Enantioconvergent C(sp³)-C(sp) Cross-coupling of Tertiary Electrophiles with Alkynes. *Nat. Chem.* **2022**, *14*, 949–957.
- (43) Cao, S.; Hong, W.; Ye, Z.; Gong, L. Photocatalytic Three-Component Asymmetric Sulfonylation via Direct C(sp³)-H Functionalization. *Nat. Commun.* **2021**, *12*, No. 2377.
- (44) Liang, Y.; Paulus, F.; Daniliuc, C. G.; Glorius, F. Catalytic Formal $[2\pi + 2\sigma]$ Cycloaddition of Aldehydes with Bicyclobutanes: Expedient Access to Polysubstituted 2-Oxabicyclo[2.1.1]hexanes. *Angew. Chem., Int. Ed.* **2023**, *62*, No. e202305043.
- (45) Tokumasu, K.; Yazaki, R.; Ohshima, T. Direct Catalytic Chemoselective α -Amination of Acylpyrazoles: a Concise Route to Unnatural α -Amino Acid Derivatives. *J. Am. Chem. Soc.* **2016**, *138*, 2664–2669.

- (46) Lin, S.-L.; Chen, Y.-H.; Liu, H.-H.; Xiang, S.-H.; Tan, B. Enantioselective Synthesis of Chiral Cyclobutenes Enabled by Brønsted Acid-Catalyzed Isomerization of BCBS. *J. Am. Chem. Soc.* **2023**, *145*, 21152–21158.
- (47) Medina, F. G.; Marrero, J. G.; Macías-Alonso, M.; González, M. C.; Córdova-Guerrero, I.; Teissier-García, A. G.; Osegueda-Robles, S. Coumarin Heterocyclic Derivatives: Chemical Synthesis and Biological Activity. *Nat. Prod. Rep.* **2015**, *32*, 1472–1507.
- (48) Trimble, J. S.; Crawshaw, R.; Hardy, F. J.; Levy, C. W.; Brown, M. J. B.; Fuerst, D. E.; Heyes, D. J.; Obexer, R.; Green, A. P. A Designed Photoenzyme for Enantioselective [2+2] Cycloadditions. *Nature* **2022**, *611*, 709–714.
- (49) (a) Xu, M.-M.; Yang, L.; Tan, K.; Chen, X.; Lu, Q.-T.; Houk, K. N.; Cai, Q. An Enantioselective Ambimodal Cross-Diels–Alder Reaction and Applications in Synthesis. *Nat. Catal.* **2021**, *4*, 892–900. (b) Lu, Y.; Xu, M.-M.; Zhang, Z.-M.; Zhang, J.; Cai, Q. Catalytic Asymmetric Inverse-Electron-Demand Diels–Alder Reactions of 2-Pyrones with Indenes: Total Syntheses of Cephanolides A and B. *Angew. Chem., Int. Ed.* **2021**, *60*, 26610–26615. (c) Si, X.-G.; Feng, S.-X.; Wang, Z.-Y.; Chen, X.; Xu, M.-M.; Zhang, Y.-Z.; He, J.-X.; Yang, L.; Cai, Q. Enantioselective Synthesis of *cis*-Decalins by Merging the Birch Reduction and Inverse-Electron-Demand Diels–Alder Reaction. *Angew. Chem., Int. Ed.* **2023**, *62*, No. e202303876.
- (50) Attard, J. W.; Noel, J. R.; Guan, Y.; Mattson, A. E. Enantioselective Access to Tetrahydroxanthenes via Copper-*bis*(oxazoline)-Catalyzed [4 + 2] Cycloaddition. *Org. Lett.* **2023**, *25*, 2450–2455.
- (51) *Flavonoids: Chemistry, Biochemistry and Applications*; Andersen, Ø. M.; Markham, K. R., Eds.; Taylor & Francis: London, 2006.
- (52) Luo, J.; Jing, D.; Lu, C.; Zheng, K. Photoinduced Metal-free Decarboxylative Transformations: Rapid Access to Amines, Alkyl Halides, and Olefins. *Eur. J. Org. Chem.* **2023**, *26*, No. e202300167.
- (53) Qin, T.; Malins, L. R.; Edwards, J. T.; Merchant, R. R.; Novak, A. J.; Zhong, J. Z.; Mills, R. B.; Yan, M.; Yuan, C.; Eastgate, M. D.; Baran, P. S. Nickel-Catalyzed Barton Decarboxylation and Giese Reactions: a Practical Take on Classic Transforms. *Angew. Chem., Int. Ed.* **2017**, *56*, 260–265.
- (54) Fawcett, A.; Pradeilles, J.; Wang, Y.; Mutsuga, T.; Myers, E. L.; Aggarwal, V. K. Photoinduced Decarboxylative Borylation of Carboxylic Acids. *Science* **2017**, *357*, 283–286.
- (55) Yang, Y.; Tsien, J.; Hughes, J. M. E.; Peters, B. K.; Merchant, R. R.; Qin, T. An Intramolecular Coupling Approach to Alkyl Bioisosteres for the Synthesis of Multisubstituted Bicycloalkyl Boronates. *Nat. Chem.* **2021**, *13*, 950–955.
- (56) Brooks, W. H.; Guida, W. C.; Daniel, K. G. The Significance of Chirality in Drug Design and Development. *Curr. Top. Med. Chem.* **2011**, *11*, 760–770.
- (57) (a) Zhao, L.; Fan, T.; Shi, Z.; Ding, C.; Zhang, C.; Yuan, Z.; Sun, Q.; Tan, C.; Chu, B.; Jiang, Y. Design, Synthesis and Evaluation of Novel ErbB/HDAC Multitargeted Inhibitors with Selectivity in EGFR^{T790M} Mutant Cell Lines. *Eur. J. Med. Chem.* **2021**, *213*, No. 113173. (b) Xiao, B.; Shi, Z.; Liu, J.; Huang, Q.; Shu, K.; Liu, F.; Zhi, C.; Zhang, D.; Wu, L.; Yang, S.; Zeng, X.; Fan, T.; Liu, Z.; Jiang, Y. Design, Synthesis, and Evaluation of VHL-Based EZH2 Degraders for Breast Cancer. *Bioorg. Chem.* **2024**, *143*, No. 107078.
- (58) (a) Wang, F.; Stappenbeck, F.; Parhami, F. Inhibition of Hedgehog Signaling in Fibroblasts, Pancreatic, and Lung Tumor Cells by Oxy186, an Oxysterol Analogue with Drug-Like Properties. *Cells* **2019**, *8*, No. 509. (b) Zhang, Y.; Vagiannis, D.; Budagaga, Y.; Sabet, Z.; Hanke, I.; Rozkoš, T.; Hofman, J. Sonidegib Potentiates the Cancer Cells' Sensitivity to Cytostatic Agents by Functional Inhibition of ABCB1 and ABCG2 in Vitro and Ex Vivo. *Biochem. Pharmacol.* **2022**, *199*, No. 115009. (c) Ma, C.; Hu, K.; Ullah, I.; Zheng, Q.-K.; Zhang, N.; Sun, Z.-G. Molecular Mechanisms Involving the Sonic Hedgehog Pathway in Lung Cancer Therapy: Recent Advances. *Front. Oncol.* **2022**, *12*, No. 729088.
- (59) (a) Rodríguez-Blanco, J.; Schilling, N. S.; Tokhunts, R.; Giambelli, C.; Long, J.; Liang Fei, D.; Singh, S.; Black, K. E.; Wang, Z.; Galimberti, F.; Bejarano, P. A.; Elliot, S.; Glassberg, M. K.; Nguyen, D. M.; Lockwood, W. W.; Lam, W. L.; Dmitrovsky, E.; Capobianco, A. J.; Robbins, D. J. The Hedgehog Processing Pathway is Required for NSCLC Growth and Survival. *Oncogene* **2013**, *32*, 2335–2345. (b) Onishi, H. Hedgehog Signaling Pathway as a New Therapeutic Target in Pancreatic Cancer. *World J. Gastroenterol.* **2014**, *20*, 2335–2342. (c) Jain, S.; Song, R.; Xie, J. Sonidegib: Mechanism of Action, Pharmacology, and Clinical Utility for Advanced Basal Cell Carcinomas. *OncoTargets Ther.* **2017**, *10*, 1645–1653.
- (60) (a) Jiang, X.-M.; Xu, Y.-L.; Huang, M.-Y.; Zhang, L.-L.; Su, M.-X.; Chen, X.; Lu, J.-J. Osimertinib (AZD9291) Decreases Programmed Death Ligand-1 in EGFR-mutated Non-small Cell Lung Cancer Cells. *Acta Pharmacol. Sin.* **2017**, *38*, 1512–1520. (b) Zhou, K.-X.; Huang, S.; Hu, L.-P.; Zhang, X.-L.; Qin, W.-T.; Zhang, Y.-L.; Yao, L.-L.; Yu, Y.; Zhou, Y.-Q.; Zhu, L.; Ji, J.; Zhang, Z.-G.; Teng, Z. Increased Nuclear Transporter KPNA2 Contributes to Tumor Immune Evasion by Enhancing PD-L1 Expression in PDAC. *J. Immunol. Res.* **2021**, *2021*, No. 6694392. (c) Zhong, B.; Zheng, J.; Wen, H.; Liao, X.; Chen, X.; Rao, Y.; Yuan, P. NEDD4L Suppresses PD-L1 Expression and Enhances Anti-tumor Immune Response in A549 Cells. *Genes Genom.* **2022**, *44*, 1071–1079.
- (61) (a) Mu, C.-Y.; Huang, J.-A.; Chen, Y.; Chen, C.; Zhang, X.-G. High Expression of PD-L1 in Lung Cancer may Contribute to Poor Prognosis and Tumor Cell Immune Escape through Suppressing Tumor Infiltrating Dendritic Cells Maturation. *Med. Oncol.* **2011**, *28*, 682–688. (b) Hu, Y.; Chen, W.; Yan, Z.; Ma, J.; Zhu, F.; Huo, J. Prognostic Value of PD-L1 Expression in Patients with Pancreatic Cancer. *Medicine* **2019**, *98*, No. e14006. (c) Cai, Y.; Xiao, M.; Li, X.; Zhou, S.; Sun, Y.; Yu, W.; Zhao, T. BMS-202, a PD-1/PD-L1 Inhibitor, Decelerates the Pro-fibrotic Effects of Fibroblasts Derived from Scar Tissues via ERK and TGFβ1/Smad Signaling Pathways. *Immun., Inflammation Dis.* **2022**, *10*, No. e693.
- (62) Zhang, J.; Su, J.-Y.; Zheng, H.; Li, H.; Deng, W.-P. Eu(OTf)₃-Catalyzed Formal Dipolar [4π+2σ] Cycloaddition of Bicyclo-[1.1.0]-butanes with Nitrones: Access to Polysubstituted 2-Oxa-3-azabicyclo[3.1.1]heptanes. *Angew. Chem., Int. Ed.* **2024**, *63*, No. e202318476.
- (63) Dron, P. I.; Zhao, K.; Kaleta, J.; Shen, Y.; Wen, J.; Shoemaker, R. K.; Rogers, C. T.; Michl, J. Bulk Inclusions of Pyridazine-Based Molecular Rotors in Tris(o-phenylenedioxy)cyclotriphosphazene (TPP). *Adv. Funct. Mater.* **2016**, *26*, 5718–5732.